Atmos. Chem. Phys., 14, 11201–11219, 2014
www.atmos-chem-phys.net/14/11201/2014/
doi:10.5194/acp-14-11201-2014


Atmospheric Chemistry and Physics Open Access

# Reactive bromine chemistry in Mount Etna's volcanic plume: the influence of total Br, high-temperature processing, aerosol loading and plume–air mixing

**T. J. Roberts**[1], **R. S. Martin**[2], **and L. Jourdain**[1]

[1]LPC2E, UMR 7328, CNRS-Université d'Orléans, 3A Avenue de la Recherche Scientifique, 45071 Orleans, CEDEX 2, France
[2]Department of Geography, University of Cambridge, Downing Place, CB2 3EN, UK

*Correspondence to:* T. J. Roberts (tjardaroberts@gmail.com)

Received: 4 December 2013 – Published in Atmos. Chem. Phys. Discuss.: 3 March 2014
Revised: 10 July 2014 – Accepted: 22 July 2014 – Published: 23 October 2014

**Abstract.** Volcanic emissions present a source of reactive halogens to the troposphere, through rapid plume chemistry that converts the emitted HBr to more reactive forms such as BrO. The nature of this process is poorly quantified, yet is of interest in order to understand volcanic impacts on the troposphere, and infer volcanic activity from volcanic gas measurements (i.e. $BrO / SO_2$ ratios). Recent observations from Etna report an initial increase and subsequent plateau or decline in $BrO / SO_2$ ratios with distance downwind.

We present daytime *PlumeChem* model simulations that reproduce and explain the reported trend in $BrO / SO_2$ at Etna including the initial rise and subsequent plateau. Suites of model simulations also investigate the influences of volcanic aerosol loading, bromine emission, and plume–air mixing rate on the downwind plume chemistry. Emitted volcanic HBr is converted into reactive bromine by autocatalytic bromine chemistry cycles whose onset is accelerated by the model high-temperature initialisation. These rapid chemistry cycles also impact the reactive bromine speciation through inter-conversion of Br, $Br_2$, BrO, $BrONO_2$, BrCl, HOBr.

We predict a new evolution of Br speciation in the plume. BrO, $Br_2$, Br and HBr are the main plume species near downwind whilst BrO and HOBr are present further downwind (where $BrONO_2$ and BrCl also make up a minor fraction). $BrNO_2$ is predicted to be only a relatively minor plume component.

The initial rise in $BrO / SO_2$ occurs as ozone is entrained into the plume whose reaction with Br promotes net formation of BrO. Aerosol has a modest impact on $BrO / SO_2$ near-downwind ($< \sim 6$ km, $\sim 10$ min) at the relatively high loadings considered. The subsequent decline in $BrO / SO_2$ occurs as entrainment of oxidants $HO_2$ and $NO_2$ promotes net formation of HOBr and $BrONO_2$, whilst the plume dispersion dilutes volcanic aerosol so slows the heterogeneous loss rates of these species. A higher volcanic aerosol loading enhances $BrO / SO_2$ in the ($> 6$ km) downwind plume.

Simulations assuming low/medium and high Etna bromine emissions scenarios show that the bromine emission has a greater influence on $BrO / SO_2$ further downwind and a modest impact near downwind, and show either complete or partial conversion of HBr into reactive bromine, respectively, yielding BrO contents that reach up to $\sim 50$ or $\sim 20$ % of total bromine (over a timescale of a few 10 s of minutes).

Plume–air mixing non-linearly impacts the downwind $BrO / SO_2$, as shown by simulations with varying plume dispersion, wind speed and volcanic emission flux. Greater volcanic emission flux leads to lower $BrO / SO_2$ ratios near downwind, but also delays the subsequent decline in $BrO / SO_2$, and thus yields higher $BrO / SO_2$ ratios further downwind. We highlight the important role of plume chemistry models for the interpretation of observed changes in $BrO / SO_2$ during/prior to volcanic eruptions, as well as for quantifying volcanic plume impacts on atmospheric chemistry. Simulated plume impacts include ozone, $HO_x$ and $NO_x$ depletion, the latter converted into $HNO_3$. Partial recovery of ozone occurs with distance downwind, although cumulative ozone loss is ongoing over the 3 h simulations.

**Published by Copernicus Publications on behalf of the European Geosciences Union.**

## 1 Introduction

The discovery of volcanic BrO (Bobrowski et al., 2003), and its subsequent observation in many volcanic plumes globally (e.g. Oppenheimer et al., 2006; Bobrowski et al., 2007; Bobrowski and Platt, 2007; Kern et al., 2009; Bani et al., 2009; Louban et al., 2009; Theys et al., 2009; Boichu et al., 2011; Heue et al., 2011; Bobrowski and Giuffrida, 2012; Rix et al., 2012; Hörmann et al., 2013; Kelly et al., 2013; Lübcke et al., 2014), demonstrates the reactivity of volcanic halogen emissions in the troposphere. Volcanoes release $H_2O$, $CO_2$ and $SO_2$, but also a range of hydrogen halides to the atmosphere including HF, HCl and HBr (in descending order of abundance in the emission, see e.g. Aiuppa et al., 2005). HF is too strong an acid for reactive halogen cycling, but for HBr and HCl, observational evidence shows these are not simply just washed out from the atmosphere, but can undergo transformation into reactive halogen species.

Notably, DOAS (differential optical absorption spectroscopy) measurements show that BrO forms at hundreds of pmol mol$^{-1}$ to nmol mol$^{-1}$ mixing ratios just minutes downwind, an order of magnitude higher than that found in the Arctic, where BrO episodes of up to tens of pmol mol$^{-1}$ cause significant ozone depletion and mercury deposition events (Simpson et al., 2007). Additionally, there is potential to use long-term BrO monitoring at volcanoes as an indicator of volcanic activity (Bobrowski and Giuffrida, 2012). Thus there is strong interest in developing models to simulate the formation of reactive bromine (and chlorine) in volcanic plumes, and to predict the downwind impacts from both quiescently degassing volcanoes and episodic eruptions to the troposphere. Studies to date usually use equilibrium models to predict the high-temperature chemistry of the near-vent plume, which is then used to initialise kinetic atmospheric chemistry models of the downwind reactive halogen chemistry (Bobrowski et al., 2007; Roberts et al., 2009; von Glasow, 2010; Kelly et al., 2013). See von Glasow et al. (2009) for an overview.

This study uses a purpose-built kinetic model, *PlumeChem* (Roberts et al., 2009), to investigate the volcanic plume reactive halogen chemistry, focusing here on bromine in a case study for Mt Etna. We include a revised methodology (Martin et al., 2009) for equilibrium calculations used to represent the near-vent high-temperature chemistry, and discuss uncertainties in the use of thermodynamic equilibrium models. Below, we outline the progression of recent research on using equilibrium models for high-temperature near-vent plume chemistry and the development of kinetic models for volcanic plume reactive halogen (BrO) chemistry. We then describe the new findings of this study specifically regarding the in-plume reactive bromine evolution presented by the model, and to highlight uncertainties in model high-temperature initialisation and the influence of total bromine, aerosol and plume–air mixing on the plume chemistry.

### 1.1 Application of the HSC equilibrium model to the near-vent plume

HSC is a commercially available model (Outotec, Finland) that predicts the thermodynamic equilibrium composition of a gas mixture at a defined temperature, pressure and chemical composition. Such models are used to represent the composition of the near-vent volcano plume (e.g. Gerlach, 2004; Martin et al., 2006), predicting a vast array ($\geq 100$) of chemical species. An overview of the input and outputs to HSC is provided in Table 1. The chemical composition of the mixture is determined by combining magmatic (comprising of $H_2O$, $CO_2$, CO, $SO_2$, $H_2S$, $H_2$, HF, HCl, HBr, HI, Hg, typically at around 800–1100 °C) and air ($N_2$, $O_2$, Ar, typically around 0–20 °C) components. The magmatic gas composition varies between volcanoes and may be estimated from crater-rim measurements. It is also possible to predict the abundance of gases that are missing from measurements as the magmatic gas $H_2O$–$H_2$, $CO_2$–CO, $SO_2$–$H_2S$ equilibria are functions of oxygen fugacity, pressure of degassing and temperature (e.g. Giggenbach, 1987). The resulting HSC output composition depends critically on the assumed ratio of air to magmatic gases in the near-vent plume, $V_A : V_M$. However, this ratio is poorly defined, an issue we examine further in this study.

The HSC output is then used to initialise low-temperature kinetic models (such as *PlumeChem*, Roberts et al., 2009; Kelly et al., 2013; *MISTRA*, Bobrowski et al., 2007; von Glasow, 2010) of the volcanic plume reactive halogen chemistry including formation of BrO. These models show that elevated radicals in the HSC output accelerate the onset of autocatalytic BrO chemistry, leading to very rapid BrO formation. BrO formation occurs more slowly in kinetic models that are not initialised with high-temperature chemistry. For the interest of atmospheric modellers, we simplify the complex HSC output ($\geq 100$ species) in Table 1, following Roberts et al. (2009) who identified impacts of $HO_x$, $NO_x$, $Br_x$ and $Cl_x$ on the downwind plume halogen chemistry. Key species are identified to be OH, NO, Br, Cl and $Cl_2$, noting $NO_2 \ll NO$ and $HO_2 \ll OH$, $Br_2 \ll Br$ in the HSC output. These species act to accelerate autocatalytic reactive bromine formation (see Fig. 4 of Roberts et al., 2009). High-temperature near-vent formation of $SO_3$ (a precursor to $H_2SO_4$) also influences the volcanic plume halogen chemistry by providing a source of aerosol surface area.

However, the thermodynamic assumption behind equilibrium models such as HSC may not always be appropriate for volcanic plume applications: Martin et al. (2009) noted that the near-complete re-equilibration (i.e. oxidation) of $H_2S$ within HSC is in disagreement with the widespread observed presence of $H_2S$ in volcanic plumes (exception: Erebus), and suggested a revised operation of HSC in which $H_2S$ is removed prior to re-equilibration. Furthermore, recent measurements confirming volcanic $H_2$ (Aiuppa et al., 2011; Roberts et al., 2012) indicate that this argument also applies

**Table 1.** Thermodynamic modelling of the high-temperature near-vent plume using HSC: overview of inputs and outputs.

| HSC input: chemical | Comments |
|---|---|
| $H_2O$, $CO_2$, $SO_2$ | Major volcanic gases |
| HF, HCl, HBr, HI | Halogen emissions |
| $H_2S$, CO, $H_2$ | Reduced gases |
| Hg | Trace metals |
| $N_2$, $O_2$, Ar | Air |
| **HSC input: physical** | |
| $V_A : V_M$ | Atmospheric : magmatic gas ratio |
| Temperature | Magmatic and ambient temperature |
| **HSC output:** | |
| Full matrix of species | (*see footnote) |
| **Key reactive species in output:** | |
| NO, OH, Cl, Br, $Cl_2$ | Species that act to kick-start BrO chemistry |
| $SO_3$ | Sulfur trioxide: direct precursor to sulfuric acid $H_2SO_4$ (or $SO_4^{2-}$: sulfate) |
| **Major volcanic gases in output:** | |
| $SO_2$, HCl, HBr, $CO_2$, $H_2O$ | Present in plume and in HSC output |
| $H_2S$, $H_2$, CO | Present in plume but missing in HSC output |

* Full matrix of species typically included in HSC output:
$H_2O$, $N_2$, $CO_2$, $SO_2$, $H_2$, HCl, $O_2$, $H_2S$, CO, Ar, $S_2$, $SO_3$, SO, NO, HBr, COS, HS, OH, Cl, Br, $S_2O$, $H_2S_2$, $Cl_2$, I, HOCl, $S_3$, HI, HF, H, $H_2SO_4$, BrCl, $NO_2$, S, ClO, O, $HO_2$, $Br_2$, HIO, $H_2O_2$, $HNO_2$, SOCl, ICl, HCOOH, $CS_2$, BrO, $S_2Cl$, $N_2O$, NOCl, $HSO_3Cl$, IBr, SCl, $S_4$, IO, NOBr, COOH, HNO, $NH_3$, ClOO, $S_5$, $SCl_2$, CH4, $HNO_3$, HCO, BrOO, CS, OClO, $O_3$, $I_2$, $ClO_2$, $SBr_2$, HClCO, $SOCl_2$, ClClO, ClOCl, NOI, $NO_2Cl$, $SO_2Cl_2$, SOF, IOO, $HSO_3F$, ClOCl, SN, COCl, $NO_3$, $S_2Cl_2$, OBrO, $S_6$, F, NBr, HOCN, HNCO, BrOBr, $CH_3$, ClF, HCN, $COCl_2$, $N_2O_2$, BrF, $NH_2$, OIO, IF, N, BrBrO, $S_2Br_2$, NOF, IIO, $N_2O_3$, $NH_2OH$, $SO_2ClF$, SF.

to $H_2$, as well as CO (although CO is typically present in low concentrations, with some exceptions, e.g. Mt Erebus). See e.g. Gerlach (2004) for various collated emission compositions. Uncertainties and limitations in the use of HSC to represent the near-vent plume composition are discussed further in this study in the context of downwind BrO chemistry.

### 1.2 Kinetic models of downwind volcanic plume reactive halogen chemistry

Atmospheric chemistry models have been developed in an effort to simulate the reactive halogen chemistry of volcanic plumes, explain observed BrO formation and predict impacts of reactive volcanic halogens on atmospheric chemistry. To date, two models: *MISTRA* (that simulates an advected column of air, Bobrowski et al., 2007) and *PlumeChem* (in an expanding box or multi-grid box modes, Roberts et al., 2009) have been developed for this purpose. Initialisation of these models includes the high-temperature chemistry of the near-vent plume, as represented by HSC. Calculations by Oppenheimer et al. (2006) showed BrO formation to be too slow if high-temperature near-vent radical formation is ignored. Bobrowski et al. (2007) performed the first *MISTRA* kinetic model simulations of volcanic plume reactive halogen chemistry, using a model initialised with HSC at $V_A : V_M$ of 0 : 100, 15 : 85, 40 : 60, finding that the 40 : 60 simulation yielded highest downwind $BrO / SO_2$. Roberts et al. (2009) queried the use of such high $V_A : V_M$ of 40 : 60 which yields rather high $SO_3 : SO_2$ ratios, that implies volcanic sulfate emissions would exceed volcanic $SO_2$. Roberts et al. (2009) presented model simulations initialised with HSC at $V_A : V_M$ of 10 : 90 that reproduced the rapid formation of $BrO / SO_2$ at a range of Arc (subduction zone) volcanoes for the first time (including Etna, Soufrière Hills, Villarrica), and suggested the higher $BrO / SO_2$ observed in the Soufrière Hills volcano plume may be fundamentally due to higher Br / S in the emission. A model study by von Glasow (2010) with simulations initialised at $V_A : V_M$ of 15:85 demonstrated good agreement to both reported column abundances of $SO_2$ and $BrO / SO_2$ ratios downwind of Etna.

All of the above-mentioned simulations (Bobrowski et al., 2007; Roberts et al., 2009; von Glasow, 2010) predict substantial in-plume depletion of oxidants, including ozone, although to varying extents, and predict contrasting plume halogen evolution. Roberts et al. (2009) also demonstrated conversion of $NO_x$ into nitric acid via $BrONO_2$, and proposed this mechanism to explain reported elevated $HNO_3$ in volcano plumes. Von Glasow (2010) simulated the impacts of volcanic reactive halogen chemistry on mercury speciation, predicting significant conversion to $Hg^{II}$ in the plume.

A number of observations of ozone abundance in volcanic plumes have recently been reported: Vance et al. (2010) observed ozone depletion in the Eyjafjallajökull plume, and at ground-level on Etna's flanks (by passive sampling).

Schumann et al. (2011) presented multiple measurements of the downwind plume of Eyjafjallajökull that observed ozone depletion to variable degrees. There exist also observations of depleted ozone in the Mount St Helens plume (Hobbs et al., 1982) that are now believed to be likely due to BrO chemistry. Ozone depletion of up to $\sim 35\,\%$ was reported in an aircraft study of Mt Erebus plume in Antarctica (Oppenheimer et al., 2010), where BrO has also been observed (Boichu et al., 2011). A systematic instrumented aircraft investigation of ozone depletion in a volcano plume (where emissions are also quantified) is presented by Kelly et al. (2013), and compared to *PlumeChem* model simulations over 2 h of plume evolution, finding good spatial agreement in the modelled and observed ozone mixing ratios. At higher altitudes, ozone depletion in a volcanic plume is reported in the UTLS (upper troposphere, lower stratosphere) region observed by Rose et al. (2006), and investigated and attributed to reactive halogen chemistry by Millard et al. (2006).

However, ozone depletion has not been universally observed: Baker et al. (2011) did not detect an ozone depletion signal relative to the (somewhat variable) background level during an aircraft transect through Eyjafjallajökull plume. An instrumented aircraft study found no evidence for $O_3$ depletion in the plume of Nevado del Huila (Colombia) and found ozone levels 70–80 % of ambient in the plume of Tungurahua (Ecuador), which could not be conclusively attributed to BrO chemistry (Carn et al., 2011).

A number of modelling discrepancies also exist. For example, the model studies of Roberts et al. (2009), von Glasow (2010) and Kelly et al. (2013) predict contrasting Br speciation and contrast in predicted impacts on ozone and other oxidants. This may reflect differences in the model representations and modelling uncertainties or demonstrate volcano-specific differences in the plume chemistry. Navigating the vast model parameter space of volcanic plume chemistry is challenging due to the non-linear controls on the plume chemistry of multiple inter-dependent parameters including volcanic aerosol, rate of horizontal dispersion, rate of vertical dispersion, wind speed, volcanic gas flux, bromine in the emission and high-temperature radical formation. Limited observational data sets are available to compare to the models, and the available data do not fully constrain the high- and low-temperature plume chemistry. To provide further insight, this study presents new *PlumeChem* model simulations to compare to recently reported trends in $BrO\,/\,SO_2$ ratios, and illustrates several of the major controls and uncertainties in the reactive halogen chemistry of volcanic plumes.

## 2 Methods

### 2.1 HSC: equilibrium modelling of near-vent plume chemistry

The use of HSC for calculating the composition of the near-vent plume is described by Gerlach (2004) and Martin et al. (2006). This study uses HSC thermodynamic model version 7.1, and applies the modifications which were proposed by Martin et al. (2009). A simple background atmosphere of $N_2$ (78 %), $O_2$ (21 %) and Ar (1 %) is assumed for the HSC calculations. The magmatic composition used for Etna follows that of Bagnato et al. (2007), with gas mixing ratios for $H_2O$, $CO_2$, $SO_2$, HCl, $H_2S$, $H_2$, CO, of 0.86, $9.6 \times 10^{-2}$, $2.9 \times 10^{-2}$, $1.4 \times 10^{-2}$, $1.5 \times 10^{-3}$, $3.7 \times 10^{-4}$ and $3.5 \times 10^{-4}$ respectively. Hg is excluded for the purposes of this study due to low abundance in the volcanic emission. The bromine content as HBr, was set to be either medium, high or low. "Medium" bromine (molar mixing ratio of $2.16 \times 10^{-5}$, equivalent to a total bromine to $SO_2$ ratio ($Br_{tot}\,/\,SO_2$) in the emission of $7.4 \times 10^{-4}$) corresponds to the average Br / S molar ratio at Etna northeast crater determined from filter-pack measurements over 2004, Aiuppa et al. (2005). "High" bromine (mixing ratio of $7.03 \times 10^{-5}$, equivalent to $Br_{tot}\,/\,SO_2$ in the emission of $2.4 \times 10^{-3}$) corresponds to that assumed in a previous model study of Etna (von Glasow, 2010), and is in the upper range (within one standard deviation) of the observations of Aiuppa et al. (2005). Simulations are also performed at a "lower" $Br_{tot}\,/\,SO_2 = 4.8 \times 10^{-4}$ which corresponds to a filter-pack Br / S measurement at Voragine crater reported by Oppenheimer et al. (2006). These are summarised in Table 2.

The magmatic temperature is set to 1050 °C in order to match that prescribed by von Glasow (2010), although we note that Metrich and Rutherford (1998) estimated Etna magmatic temperature to be 1100 °C. For the near-vent plume mixture input to HSC, ambient air temperature was set to 20 °C. This is somewhat high considering Etna's elevation (3 km), but this has a minor influence on the HSC output (especially considering 50 °C difference in the magmatic temperature estimates outlined above). For the actual *PlumeChem* atmospheric chemistry model runs, the atmospheric temperature was a more realistic 285 K. The equilibrium composition was calculated for standard operation of HSC (in which $H_2$ and $H_2S$ are allowed to re-equilibrate) and in a revised (Martin et al., 2009) operation of HSC (in which $H_2$ and $H_2S$ are replaced by inert Ar such that they do not re-equilibrate). The HSC calculations were performed over 16 different $V_A : V_M$ ranging from 0 : 100 to 15 : 85.

**Table 2.** Parameters varied in *PlumeChem* sensitivity studies.

| Parameter | Values |
|---|---|
| HSC $V_A : V_M$ | 0 : 100 |
| | 2 : 98 |
| | 5 : 95 |
| | 10 : 90 |
| | 15 : 85 |
| Aerosol loading: $\mu m^2$ molec$^{-1}$ $SO_2$ | |
| High | $10^{-10}$ |
| Medium | $10^{-11}$ |
| $Br_{tot}$ / $SO_2$: molar ratio | |
| Medium | $7.4 \times 10^{-4}$ |
| High | $2.4 \times 10^{-3}$ |
| Low | $4.8 \times 10^{-4}$ |
| Gas Flux kg s$^{-1}$ $SO_2$ | |
| (small variations) | 10, 20 |
| (large variations) | 10, 50, 100 |
| Wind-speed, m s$^{-1}$ | 3, 5, 10, 15 |
| Dispersion | B, C, D |
| Pasquill–Gifford cases | |

## 2.2 PlumeChem: kinetic model of downwind BrO chemistry

The *PlumeChem* model simulates the reactive halogen chemistry of volcanic plume, as described by Roberts et al. (2009). It can be run in single-box (Roberts et al., 2009) or multi-box (Kelly et al., 2013) modes. Here we used the single box that expands as a background atmosphere is entrained into it, representing dispersion of the plume as it is advected downwind. *PlumeChem* includes a background atmospheric chemistry scheme and bromine and chlorine reactive halogen chemistry, including photolysis, gas-phase and heterogeneous (gas–aerosol) phase reactions. Autocatalytic formation of BrO occurs through cycles involving reaction of BrO with oxidants, ($HO_2$ $NO_2$), (Reactions R1, R2), aerosol-phase heterogeneous chemistry (Reactions R3, R4) to release a halogen dimer, whose photolysis generates two halogen radicals (Reaction R5), which may react with ozone (Reaction R6) to form BrO. The heterogeneous reactive uptake of HOBr and $BrONO_2$ on volcanic aerosol are thus key drivers of reactive halogen formation. Within the volcanic aerosol, aqueous-phase equilibria (Wang et al., 1994) control the nature of the product, which is $Br_2$ for a typical volcanic plume composition, thereby enabling autocatalytic formation of reactive bromine. Once aerosol $Br^-_{(aq)}$ becomes depleted (as a consequence of the BrO formation cycles), BrCl becomes a significant product from the heterogeneous Reactions (R3, R4), leading to non-autocatalytic formation of reactive chlorine. Repeated cycling around Reactions (R1–R6) can cause substantial ozone loss (orders of magnitude greater than the BrO mixing ratio). Repeated cycling between BrO and Br (Reactions R6, R7) further enhances ozone loss in concentrated plume environments:

$$BrO + HO_2 \rightarrow HOBr + O_2 \quad \text{(R1)}$$

$$BrO + NO_2 \rightarrow BrONO_2 \quad \text{(R2)}$$

$$HOBr + H^+_{(aq)} + Br^-_{(aq)} \rightarrow Br_{2(aq \rightarrow g)} + H_2O \quad \text{(R3)}$$

$$BrONO_2 + H_2O_{(l)} \rightarrow HOBr + HNO_3 \quad \text{(R4)}$$

$$Br_2 \xrightarrow{h\nu} 2Br \quad \text{(R5)}$$

$$Br + O_3 \rightarrow BrO + O_2 \quad \text{(R6)}$$

$$BrO + BrO \rightarrow 2Br + O_2. \quad \text{(R7)}$$

The background atmosphere chemistry scheme used here is identical to that of Roberts et al. (2009), assuming a somewhat polluted atmosphere. For the model simulations initialised around midday, background ozone is $\sim 60$ nmol mol$^{-1}$, and $NO_x$ and $HO_x$ are around 0.17 and 30 pmol mol$^{-1}$ respectively, with an ambient temperature of 285 K and 60 % relative humidity (RH). Plume dispersion is defined according to Pasquill–Gifford dispersion schemes (see Supplement). The base-run plume dispersion parameterisation used in this study is identical to that of Roberts et al. (2009), based on Pasquill–Gifford case D, with a $SO_2$ gas flux of 10 kg s$^{-1}$ at a wind-speed of 10 m s$^{-1}$. The influence of variations in wind speed (3–15 m s$^{-1}$), volcanic emission flux (10–20 kg s$^{-1}$ $SO_2$) and dispersion rates (Pasquill–Gifford cases B, C, D) on downwind BrO / $SO_2$ ratios are also shown, as well as simulations with much greater volcanic emission flux (5 × or 10 × the base run). Volcanic aerosol loading in the model is investigated as part of the study, and for the majority of simulations is set to be $10^{-11}$ $\mu m^2$ molec $SO_2^{-1}$, a factor of 10 lower than that of Roberts et al. (2009), following the *PlumeChem* model set-up used in Kelly et al. (2013).

The reaction of Br with $BrONO_2$ to form $Br_2$+ $NO_3$ (Orlando and Tyndall, 1996) was added to the *PlumeChem* model in this study. This reaction influences the overall rate of HBr conversion into reactive bromine as follows: as a sink for $BrONO_2$ it slows the conversion of HBr into reactive bromine as less $BrONO_2$ undergoes heterogeneous uptake (which converts HBr into $Br_2$ via HOBr). However, as a sink for Br it slows the conversion of reactive bromine back into HBr from the reaction Br + HCHO. Under a high volcanic aerosol loading the former dominates, whilst the latter is more important at lower aerosol loadings. It is noted that this reaction is neither included in the IUPAC Kinetics nor JPL Data evaluation databases, thus is not necessarily included "as standard" in all atmospheric models of reactive halogen chemistry.

$BrNO_2$ was suggested by von Glasow (2010) to be an important reservoir for Br in the near-downwind plume, based on the assumed formation of $BrNO_2$ from volcanic $NO_x$ and Br radicals at a rate that exceeds $BrNO_2$ loss via

photolysis. Formation of $BrNO_2$ was not included in previous *PlumeChem* model studies (Roberts et al., 2009; Kelly et al., 2013). Here, the fate of the products ($BrNO_2$ but also BrONO) from reaction of $Br + NO_2$ are investigated in more detail to evaluate the potential of $BrNO_2$ to influence the plume chemistry.

## 3 Results

### 3.1 Model $SO_2$ column abundance, and variability in simulated $BrO / SO_2$

The formation of volcanic BrO is typically reported relative to $SO_2$, which, given slow in-plume oxidation, acts as a plume tracer on the observation timescales (typically minutes to hours). Therefore, prior to comparing *PlumeChem* model output to the observed $BrO / SO_2$, a comparison is made between the simulated and reported $SO_2$ column abundances. Figure 1a shows slant $SO_2$ column abundance in Mt Etna's plume over 2004–2005, reported from DOAS (Differential Optical Absorption Spectroscopy) observations from Oppenheimer et al. (2006) and Bobrowski et al. (2007). The data show a general decline with distance downwind, with the exception of two very near source measurements, which may have been underestimated in the very strong near-source plume, see discussion by Kern et al. (2012) and Bobrowski and Guiffrida (2012) for improved $SO_2$ evaluation. Also shown in Fig. 1a is the model downwind plume $SO_2$ column abundance calculated for the plume in the vertical. The decline in modelled $SO_2$ column abundance with distance (or time) downwind is largely due to dispersion, given the slow rate of in-plume $SO_2$ oxidation. The rate of dispersion depends on plume depth, width, gas flux and wind speed during each DOAS measurement, which are not fully constrained by available observations. Nevertheless, the broad agreement between model and observations indicates a suitable model parameterisation of plume–air mixing in the base run. This supports the use of further simulations to investigate the plume halogen chemistry using this plume–air mixing parameterisation scenario, for comparison to reported $BrO / SO_2$ observations.

Figure 1b shows formation of BrO (relative to plume tracer $SO_2$) for a range of model simulations presented later in this study, all using this same plume–air mixing parameterisation, but where the other parameters (volcanic aerosol loading, total plume bromine, initialisation using thermodynamic model output) are varied. Clearly, these variables can have a strong influence on the downwind plume halogen chemistry. Also shown are $BrO / SO_2$ ratios reported by Oppenheimer et al. (2006) and the observed trend in (mean) $BrO / SO_2$ with distance downwind reported by Bobrowski et al. (2007). Several, but not all of the model simulations in Fig. 1b conform to the $BrO / SO_2$ observations. Indeed, simulations whose initialisations assume no plume–air mixing at high temperature

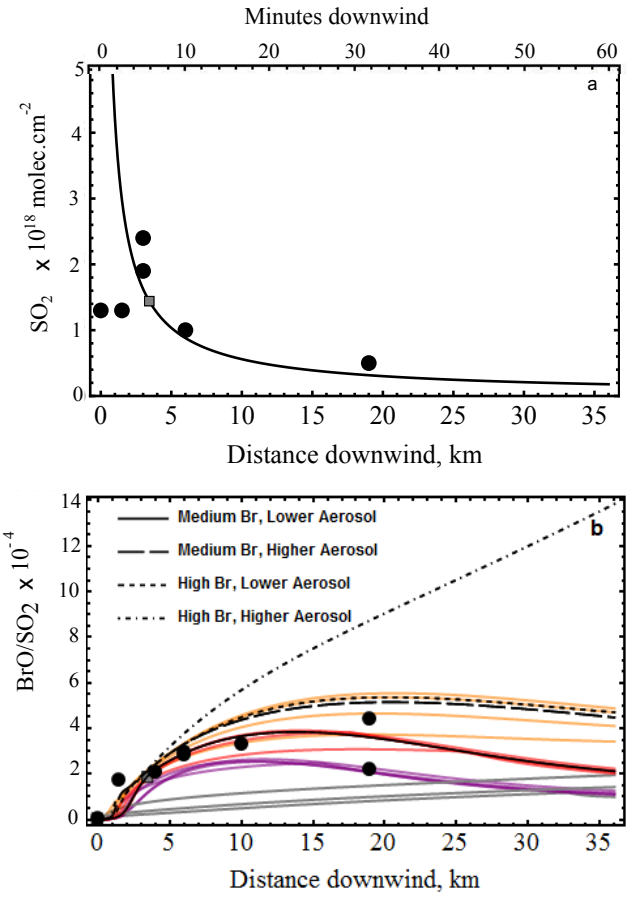


**Figure 1.** *PlumeChem* simulations illustrating **(a)** predicted $SO_2$ column abundance in the downwind plume (black line) according to the model dispersion parameterisation, **(b)** simulated downwind $BrO / SO_2$ ratios for model runs using this dispersion parameterisation but where bromine in the emission ($Br_{tot} / SO_2$), volcanic aerosol loading and the high-temperature initialisation are varied. The simulations are compared to DOAS $SO_2$ column abundances and (mean) $BrO / SO_2$ ratios reported by Oppenheimer et al. (2006), and Bobrowski et al. (2007), grey squares and black discs, respectively. Simulations with varying aerosol emission (for two bromine scenarios) are highlighted in black. Simulations assuming medium aerosol loading and varying bromine emission (for a range of plausible high-temperature model initialisations) are shown in red, orange and purple for medium, high and low Br emission scenarios, respectively. Simulations assuming no plume–air mixing in the high-temperature initialisation ($V_A : V_M = 0 : 100$) are shown in grey.

typically underestimate downwind $BrO / SO_2$ (see Sect. 3.3 for further discussion). The remaining model runs demonstrate broad agreement with the $BrO / SO_2$ measurements and provide an explanation for the observed rise and subsequent plateau or decline in $BrO / SO_2$ with distance downwind reported by Bobrowski and Giuffrida (2012).

In order to provide further insight into the factors controlling volcano plume reactive halogen chemistry, we investigate here the influence of the above-mentioned variables, and

particularly uncertainties regarding the initialisation by HSC. To do so, suitable values for the volcanic bromine and aerosol loading are first identified, as outlined below.

### 3.2 The effect of aerosol and bromine content on downwind $BrO / SO_2$

Highlighted in black in Fig. 1b are four model runs that assume the "medium" and "high" bromine ($Br_{tot} / SO_2$) emission scenarios (see Table 2), and two contrasting aerosol surface area loadings – namely "high" aerosol estimated as $\sim 10^{-10}$ µm$^2$ molec $SO_2^{-1}$ following Roberts et al. (2009), and the "medium" aerosol estimate, which is an order of magnitude lower, $10^{-11}$ µm$^2$ molec $SO_2^{-1}$ as used by Kelly et al. (2013). Both the volcanic aerosol loading and volcanic bromine content influence the downwind $BrO / SO_2$ evolution, as follows.

In general, a higher $Br_{tot} / SO_2$ in the emission leads to greater $BrO / SO_2$ far downwind. This is in accordance with the proposed role of Br / S in the emission to explain order of magnitude variation in $BrO / SO_2$ ratios across Arc volcanoes (Roberts et al., 2009). A higher aerosol loading promotes the conversion of HBr into reactive forms, and promotes the occurrence of reactive bromine as BrO in the far-downwind plume to its role in the heterogeneous reactive uptake of HOBr and $BrONO_2$. Interestingly, whilst the volcanic aerosol and bromine content have a strong impact on the plateau in $BrO / SO_2$ far downwind (both in terms of value and when it is reached), Figure 1b indicates that aerosol and bromine content exert a much more limited impact on $BrO / SO_2$ in the very young plume during the first $\sim 8$ min ($\sim 5$ km) of plume evolution, at least for the plume dispersion conditions simulated. For example, at 36 km downwind, the two contrasting aerosol loadings cause the model $BrO / SO_2$ to vary from $4.2. \times 10^{-4}$ to $1.4 \times 10^{-3}$ ("high" bromine scenario) and from $2 \times 10^{-4}$ to $4. \times 10^{-4}$ ("medium" bromine scenario), whereas at 6 km downwind all of these model runs predict $BrO / SO_2$ between $2.5 \times 10^{-4}$ and $4 \times 10^{-4}$. This near-downwind similarity in $BrO / SO_2$ (despite varying $Br_{tot} / SO_2$ as well as aerosol loading) is related to the role of oxidants in forming BrO, and differences in the proportion of HBr converted to reactive bromine. This predicted near-downwind independence of $BrO / SO_2$ on aerosol loading is consistent with the observations of Bobrowski and Giuffrida (2012) at 6 km downwind that showed $BrO / SO_2$ was independent of relative humidity (a key control on sulfate aerosol volume hence surface area). A model explanation (see Sect. 3.4 for further discussion) is that near-downwind $BrO / SO_2$ ratios are primarily controlled by Br to BrO partitioning – itself a function of in-plume ozone mixing ratio – in this region where the plume is still relatively concentrated. See Sect. 3.4 for details of the plume reactive bromine speciation and Sect. 3.6 for further discussion on the plume impacts on atmospheric ozone.

Notably, the simulation with both "high" bromine and the larger aerosol estimate predicts $BrO / SO_2$ that exceeds reported observations far downwind, and does not reproduce the plateau in $BrO / SO_2$ beyond $\sim 5$ km downwind of Etna summit recently reported by Bobrowski and Giuffrida (2012). We acknowledge the Etna bromine emission may vary with time and therefore use both medium and high bromine emission scenarios alongside a low Br scenario in the further model simulations of this study. However, for the high-bromine scenario, only the simulation with "medium" aerosol surface area loading appears consistent with the $BrO / SO_2$ observations by Bobrowski and Giuffrida (2012). The "medium" aerosol surface area loading is considered as likely being more representative and this estimate, $\sim 10^{-11}$ µm$^2$ molec $SO_2^{-1}$, is used in all further model simulations of this study. Further discussion on estimates of the aerosol surface area loading is provided in the Supplement.

### 3.3 The high-temperature near-vent plume – a source of model uncertainty

An important model parameter in the *PlumeChem* model initialisation is the use of output from thermodynamic model HSC to represent the composition of the high-temperature near-vent plume. Figure 2 illustrates the key species in the HSC output (Table 1) for the near-vent plume of Etna ("medium" Br scenario) using (a) the standard HSC methodology in which $H_2$ and $H_2S$ re-equilibrate, and (b) the modified method (Martin et al., 2009) whereby $H_2S$ and $H_2$ do not re-equilibrate. NO, OH, Cl and Br and $Cl_2$ gas mixing ratios are shown for $V_A : V_M$ ranging from 0 : 100 to 15 : 85, where $V_A : V_M$ is the ratio of air to magmatic gases in the near-vent plume (plotted as a fraction in Fig. 2), with the HSC temperature varied according to the mixture of magmatic (1050 °C) and ambient (20 °C) temperatures.

Of note is a step increase in radical mixing ratios in Fig. 2a (in which $H_2$ and $H_2S$ re-equilibrate). This is the so-called compositional discontinuity, CD (Gerlach, 2004), which occurs at around $V_A : V_M \sim 0.01$ for Etna's magmatic composition. At the CD, the reduced magmatic gases ($H_2S$, $H_2$, CO, etc.) are essentially fully oxidised ($SO_2$, $H_2O$, $CO_2$), thus addition of further oxidant (increasing $V_A / V_M$) yields increases in the mixing ratios of the radicals (Br, Cl, NO, OH). As $V_A : V_M$ increases further, the greater proportion of air relative to magmatic gases yields a lower HSC temperature, leading to slight declines or a plateau in the mixing ratios of NO and OH, and altering the balance between $Cl_2$ and Cl radicals ($Br_2$ remains low over the whole $V_A : V_M$ range). Formation of Br with increasing $V_A : V_M$ also leads to a corresponding decrease in its "parent" or "source" species HBr (note that other "parent" species, e.g. HCl, $H_2O$, are in excess relative to $Cl_x$ and OH). However, in the revised HSC methodology the CD has shifted to low $V_A : V_M$, as first shown by Martin et al. (2009). Indeed, it may no longer be

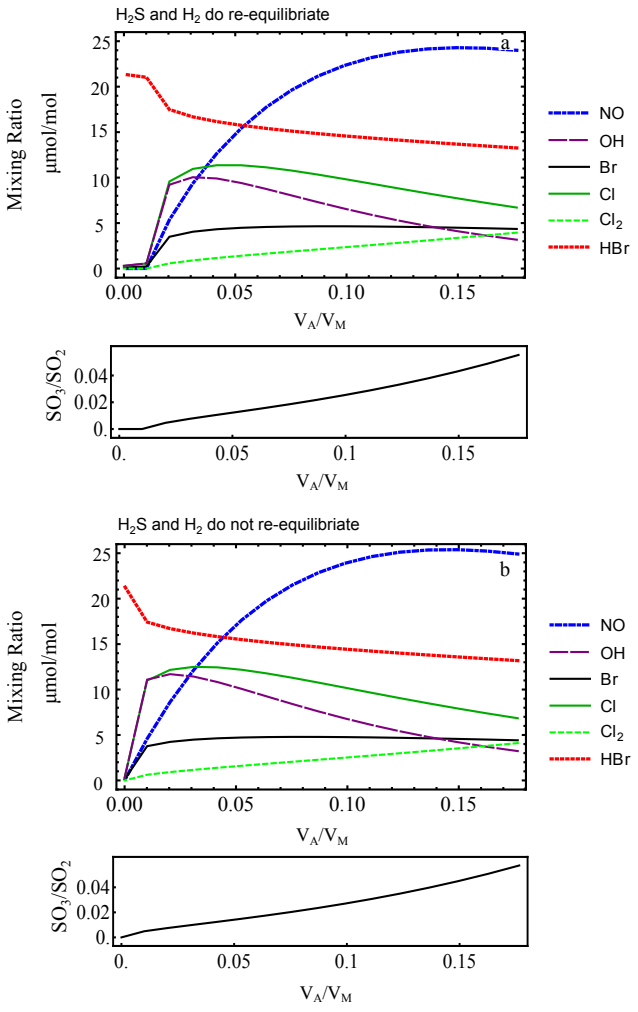


**Figure 2.** Mixing ratio ($10^{-6}$ mol mol$^{-1}$) of key species (NO, OH, Br, Cl, $Cl_2$) in the HSC output as a function of $V_A$ / $V_M$, the assumed magmatic–atmospheric gas ratio in the near-vent plume, ranging from 0 (0.00 : 1.00) to 0.18 (0.15 : 0.85). The $SO_3 : SO_2$ ratios (that prescribe the volcanic sulfate / $SO_2$ emission) in the HSC output are also shown. **(a)** Standard operation of HSC in which volcanic $H_2S$ and $H_2$ are allowed to re-equilibrate, yielding near-zero mixing ratios of these gases in the HSC output. **(b)** A revised operation of HSC (Martin et al., 2009) in which volcanic $H_2S$ and $H_2$ are removed (and temporarily replaced by inert Ar) such that they do not re-equilibrate within HSC.

relevant to talk of a CD at all, as an increase in radicals occurs immediately as $V_A : V_M$ is increased; this is because the composition of the mixture is no longer buffered by magmatic $H_2$ / $H_2O$ and $H_2S$ / $SO_2$ ratios.

The fact that certain species need to be "protected" from re-equilibration within presents a major limitation to the use of thermodynamic models to represent near-vent plume, as neither the choice of $V_A : V_M$, nor the protection of certain species (but not others) are fully justified on a physical basis. It is likely that some processes may be kinetics limited and thus poorly described by thermodynamic models. Studies suggest that this is indeed the case for the formation of $NO_x$ from background $N_2$ entrained into the plume (Martin et al., 2012), due to the high bond strength for $N_2$ (945 kJ mol). Nevertheless, there is some evidence for the high-temperature formation of radicals in the near-vent plume, for example in the presence of crater-rim sulfate at $SO_4^{2-} : SO_2 \sim 1 : 100$ (e.g. Mather et al., 2003; Martin et al., 2008), from which near-vent $SO_3$ production might be inferred. Further, a volcanic source of $HO_x$ is suggested by plume $H_2O_2$ observations of Carn et al. (2011), and a source of $HO_x$ and $NO_x$ is suggested by observations of $HO_2NO_2$ at Erebus (Oppenheimer et al., 2010), and elevated NO and $NO_2$ in plumes of Masaya (Mather et al., 2004) and Mt St Helens (see Martin et al., 2012, and references therein). Given the above-mentioned kinetic limitations to near-vent $NO_x$ production from entrained background air, these results imply the need for alternative explanations for $NO_x$ at volcanoes where it has been reported, and raise the possibility that volcano $NO_x$ emissions at other volcanoes (e.g. Etna) might be lower than predicted by HSC.

A representation of high-temperature radical formation in the near-vent plume is, however, necessary for the initialisation of atmospheric chemistry models of downwind BrO chemistry. The HSC model output is thus used for this purpose, despite the above-mentioned limitations. Figure 3 shows 1 h *PlumeChem* model simulations for the three bromine emission scenarios (low, medium, high), initialised using HSC operated at a range of $V_A : V_M$ varying from 0 : 100, 2 : 98, 5 : 95, 10 : 90 to 15 : 85, compared to reported BrO / $SO_2$ ratios from Oppenheimer et al. (2006) and Bobrowksi et al. (2007). Simulations initialised with $V_A : V_M$ of 0 : 100 (i.e. with no air mixed into the near-vent plume) under-predict BrO / $SO_2$ ratios compared to the observations, as has been shown previously (e.g. Bobrowski et al., 2007; Roberts et al., 2009; von Glasow, 2010) using atmospheric chemistry models. This is due to the low radical content at $V_A : V_M = 0 : 100$ as shown in Fig. 2). Previous studies therefore chose HSC initialisations using $V_A : V_M > 0 : 100$; e.g. Roberts et al. (2009) suggested $V_A : V_M = 10 : 90$, and von Glasow (2010) suggested $V_A : V_M = 15 : 85$. Given the revised location of the compositional discontinuity outlined above in Fig. 2, even lower $V_A : V_M$, e.g. $V_A : V_M = 2 : 98$ or $V_A : V_M = 5 : 95$ (shown in red), can become suitable. Further progress will require more sophisticated models to be developed, e.g. to include full kinetic representations of chemical and mixing processes.

An interesting feature of Fig. 3 is that whilst choice of HSC initialisation affects the 1 h downwind plume BrO / $SO_2$ strongly, the model runs show a degree of convergence towards the end of the model run (particularly for low/medium Br cases). Understanding the < 1 h plume chemistry is important for interpretation of flank volcano BrO / $SO_2$ observations, and is investigated further with simulations initialised using HSC with $V_A : V_M = 5 : 95$.

### 3.4 Speciation of reactive bromine in Etna plume and implications for observations of volcanic BrO

The evolution of reactive bromine speciation is also illustrated in Fig. 3 for the three bromine emission scenarios, with simulations initialised using HSC at $V_A : V_M = 5 : 95$. A number of interesting features are identified:

- $BrO / Br_{tot}$ rises rapidly in the first few minutes, but then stabilises or declines further downwind.
- HBr is fully converted to reactive bromine in the "medium" and "low" bromine simulations but only partially converted in the "high" bromine simulations.
- BrO is formed in the plume at up to 40–50 % ("medium" and "low" Br emission scenarios) or 10–20 % (high Br emission scenario) of total bromine. This difference is related to the extent of HBr conversion, as BrO reaches a similar maximum fraction ($\sim 50$ %) of reactive bromine in the three simulations.
- An increase in plume BrCl occurs when HBr becomes depleted, which is due to the aqueous-phase equilibria producing substantial BrCl in place of $Br_2$.
- HOBr and $BrONO_2$ are present in all simulations, and represent an increasing proportion of reactive bromine as the plume disperses downwind, whilst the proportion of BrO declines.

The observed and modelled trend in $BrO / SO_2$ shown in Figs. 1 and 3 is thus explained as follows: HBr is converted into reactive forms by autocatalytic bromine chemistry cycles involving volcanic aerosol, entrained atmospheric oxidants and sunlight. The HBr conversion is accelerated by radical species present in the high-temperature initialisation. The initial rise in $BrO / SO_2$ primarily reflects trends in reactive bromine speciation; entrainment of background air containing ozone into the plume, promotes greater partitioning to BrO via the reaction $Br + O_3$. Plume–air mixing is thus an important control on $BrO / SO_2$, because the dilution of volcanic components and entrainment of air alter the balance between Br and BrO, e.g. by reducing the rate of BrO loss by the self-reaction BrO + BrO (to form 2Br or $Br_2$), Reaction (R7), relative to the formation of BrO by $Br+O_3$, Reaction (R6). The subsequent decline or plateau in $BrO / SO_2$ occurs due to net conversion of reactive bromine from BrO to HOBr and $BrONO_2$ in the downwind plume (Reactions R1, R2). These species are formed at an accelerated rate in the downwind plume as it disperses and entrains background air containing oxidants ($HO_2$, $NO_2$) which react with BrO. Further, the heterogeneous loss pathways for these species are slowed in the dispersed downwind plume where volcanic aerosol is diluted. The heterogeneous reactions of HOBr and $BrONO_2$ with aerosol present a more rapid loss pathway than photolysis in the aerosol-rich environment of a volcanic

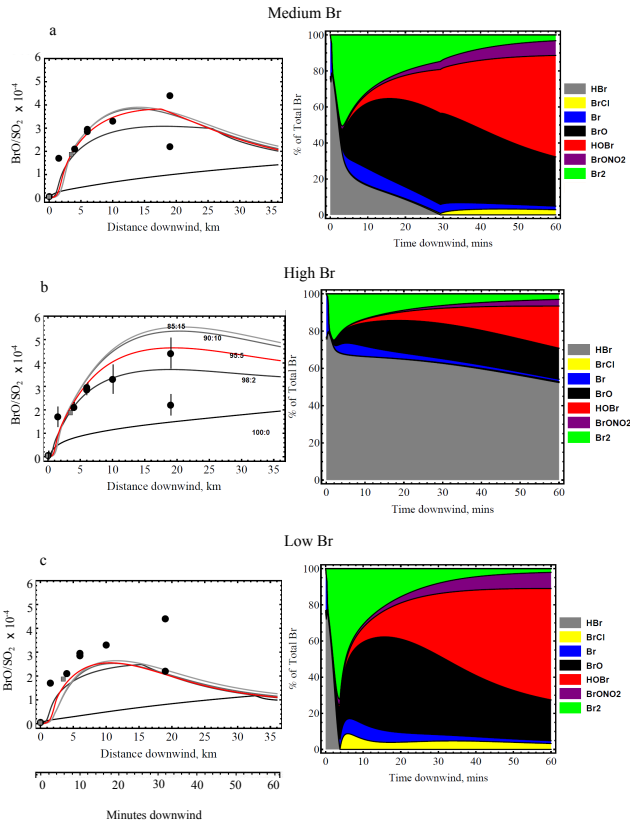


**Figure 3.** Left: simulated 1 h evolution of plume $BrO / SO_2$ for the three bromine emission scenarios, with varying atmospheric–magmatic gas ratio $V_A : V_M$ (0 : 100, 5 : 95, 10 : 90, 15 : 85) in the high-temperature initialisation. Also shown are observed $BrO / SO_2$ ratios reported by Oppenheimer et al. (2006), and Bobrowski et al. (2007); grey and black disks respectively, with representative data error bars from Bobrowski et al. (2007). Right: Br speciation for the three bromine emission scenarios shown for the model run initialised using HSC with $V_A : V_M = 5 : 95$.

plume. As the plume disperses and dilutes further downwind, net accumulation of HOBr (and $BrONO_2$) occurs whilst BrO declines (as a fraction of $Br_{tot}$), although it is emphasised that plume chemistry cycling between these species is ongoing throughout the simulation and is very rapid.

This predicted reactive bromine evolution is somewhat similar to that of Roberts et al. (2009) but contrasts to the 1 h simulations of von Glasow (2010) that did not predict the in-plume presence of HOBr and $BrONO_2$. The higher proportion of total bromine as BrO in the "medium" and "low" Br emission scenarios (40–50 %) compared to the "high" Br emission scenario (10–20 %) is related to the extent (complete and partial, respectively) of HBr conversion into reactive bromine species. This dependence of the HBr conversion on $Br_{tot} / SO_2$ in the emission may to some extent explain differences between the model studies of Roberts et al. (2009) and von Glasow (2010) that predicted complete and partial

in-plume conversion of HBr into reactive bromine, respectively.

Predicted $BrO/SO_2$ and $BrO/Br_{tot}$ trends for the three Br emission scenarios (initialised with $V_A : V_M = 5:95$) are shown in Fig. 4. The "low" Br emission scenario simulation can be compared to observations by Oppenheimer et al. (2006) who reported (using DOAS) $BrO/SO_2$ ratios reached $\sim 2 \times 10^{-4}$ within 3–4 min downwind of Etna summit, and used filter packs to quantify the emitted $Br_{tot}/SO_2$ to be $4.8 \times 10^{-4}$, implying a $BrO/Br_{tot}$ of $\sim 40\,\%$. For the "low" Br model run initialised at $Br_{tot}/SO_2 = 4.8 \times 10^{-4}$, which predicts complete conversion of HBr into reactive forms over 4 min, $BrO/SO_2$ rises to $10^{-4}$ within 4 min, reaching a maximum of $2.5 \times 10^{-4}$ at about 18 min downwind (i.e. earlier than the "medium" and "high" bromine cases of this study) after which $BrO/SO_2$ declines, Fig. 4a. $BrO/Br_{tot}$ reaches 25 % within 4 min, and 40 % by about 8 min (Fig. 4b), thus converging towards the observations of Oppenheimer et al. (2006): the agreement is relatively good considering that the predicted $BrO/Br_{tot}$ can also be affected by other model parameters kept constant here, e.g. in HSC initialisation, rate of plume–air mixing and aerosol loading, whilst observations of $BrO/Br_{tot}$ are subject to measurement uncertainties, e.g. in filter-pack Br / S, DOAS measurement of $BrO/SO_2$.

The non-linearity of HBr conversion to BrO shown in Fig. 4 yields the following implications for volcanology: $BrO/SO_2$ ratios for these simulations (initialised at $V_A : V_M = 5:95$) reach maxima of $3.6 \times 10^{-4}$ and $4.6 \times 10^{-4}$ and $2.5 \times 10^{-4}$ for the medium, high and low Br scenarios respectively in the downwind plume. Thus, whilst the modelled bromine emission has varied by a factor of three between the "medium" and "high" bromine scenarios, the simulated $BrO/SO_2$ ratio has varied by less than 30 %. This result for small-scale bromine variations contrasts to the earlier *PlumeChem* simulations (Roberts et al., 2009) which suggested that order of magnitude differences in $BrO/SO_2$ between Soufrière Hills volcano ($BrO/SO_2 \sim 10^{-3}$) and other Arc volcanoes like Etna ($BrO/SO_2 \sim 10^{-4}$) could be attributed to order of magnitude differences in the ratio of total bromine to $SO_2$ in their emissions. However, the non-linear relationship between BrO and emitted HBr, as identified in Fig. 4 for small-scale bromine variations, presents a complexity to efforts to quantify volcanic bromine emissions using DOAS observations of plume $BrO/SO_2$ ratios within volcano monitoring programmes, and to modelling efforts to quantify impacts from volcanic halogen emissions to the troposphere. Nevertheless, DOAS observations (e.g. Bobrowski et al., 2003; Bobrowski and Platt, 2007) do suggest a positive correlation between $BrO/SO_2$ and volcanic HBr emissions. For Soufrière Hills volcano, where high Br / S in the emission was proposed to lead to high plume $BrO/SO_2$, further aspects to consider include the low-altitude emission where ambient humidity and background aerosol might be high, potentially promoting both BrO chemistry and $SO_2$ oxidation rates.

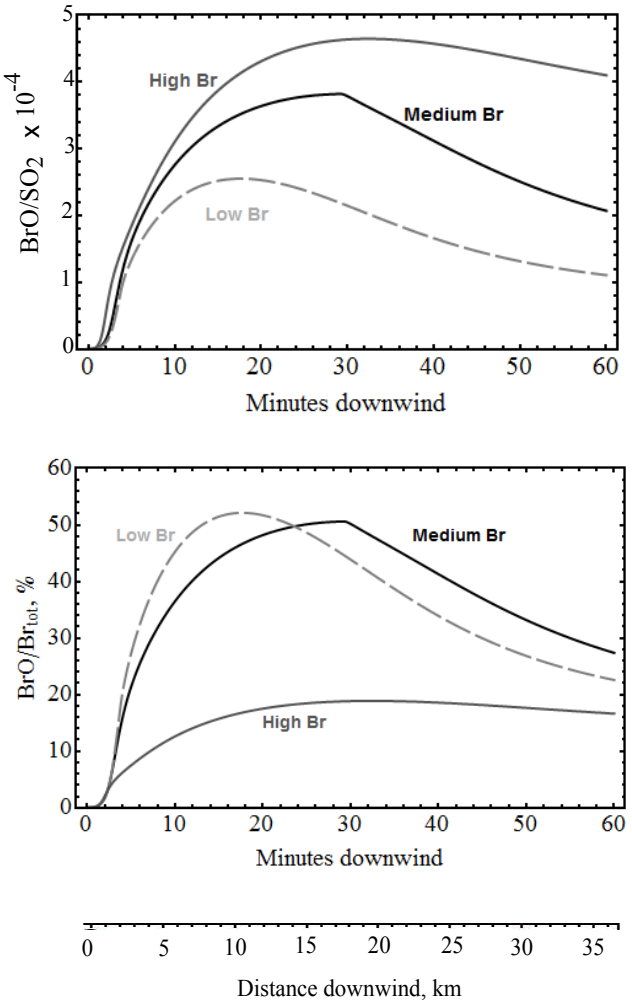


**Figure 4.** Predicted evolution in $BrO/SO_2$ (top) and $BrO/Br_{tot}$ ratios (bottom) over 1 h for the three different bromine emission scenarios. Model runs correspond to those shown in Fig. 3 assuming $V_A : V_M = 5:95$ for the high-temperature initialisation.

Further understanding of the extent to which volcanic bromine is rapidly converted into reactive forms in the near-downwind plume is needed as part of efforts to evaluate global impacts from volcanic halogen degassing. Further studies of the wider model parameter space can contribute to this aim, although more observations are also needed to constrain model uncertainty. Overall, the model suggests that HBr conversion into reactive bromine depends on a balance between the autocatalytic "bromine explosion" cycles in the near-downwind plume (accelerated by radicals produced in the high-temperature near-vent plume), and the conversion of reactive bromine back into HBr (e.g. via the reaction Br + HCHO).

### 3.5 Low in-plume prevalence of $BrNO_2$

Formation of $BrNO_2$ from Br + $NO_2$ was excluded from the 1 h simulations presented in Figs. 3 and 4. However, the plume chemistry modelling study of von Glasow (2010) predicted high in-plume prevalence of $BrNO_2$, due to reaction of Br with $NO_2$, given that high Br and $NO_x$ mixing ratios are assumed in the (HSC) model initialisation. In the Etna simulations of von Glasow (2010), formation of $BrNO_2$ exceeds its photolytic loss rate in the young plume, leading to a significant partitioning (> 30 %) of plume bromine as $BrNO_2$. To further evaluate this model difference, a similar two-reaction scheme for $BrNO_2$ was introduced into the *PlumeChem* model, with $BrNO_2$ the assumed (sole) product of the reaction Br + $NO_2$. With this two-reaction scheme, model runs for the three bromine scenarios also show rapid formation of $BrNO_2$ (Fig. 5a, c, d). The in-plume $BrNO_2$ prevalence (< 30 % of plume bromine declining to just a few percent after 30 min), is still somewhat less than that of von Glasow (2010), and model differences remain in Br speciation regarding presence of HOBr and $BrONO_2$, potentially due to differences between the models' aerosol loading or dispersion schemes. Figure 5a, c, d highlight that the rapid formation of $BrNO_2$ in these model runs causes a slight delay to the formation of BrO downwind compared to the standard model runs of Fig. 3.

However, we do not recommend use of the two-reaction $BrNO_2$ scheme, because the chemistry is in fact more complex. Firstly, the reaction Br + $NO_2$ primarily produces BrONO (∼ 92 %) rather than $BrNO_2$ (∼ 8 %) (Bröske and Zabel, 1998; Orlando and Burkholder, 2000). Secondly, BrONO undergoes a more rapid thermal dissociation ($\tau \sim 1$ s at room temperature), and photolytic loss ($\tau \sim$ seconds) than $BrNO_2$ (Burkholder and Orlando, 2000). BrONO and $BrNO_2$ also react with $NO_2$ (Bröske and Zabel, 1998). BrONO (and possibly also $BrNO_2$) also react with Br radicals. The reactions are summarised in Table 3. *PlumeChem* simulations using a more detailed reaction scheme for $BrNO_2$–BrONO–BrNO, incorporating the quantified reactions of Table 3, are illustrated in Fig. 5b, d, f. With this revised $BrNO_2$–BrONO–BrNO model scheme, these species account for only < 12 % of reactive bromine (with BrONO and BrNO at only < 1 %). The impact of this scheme on Br speciation is rather modest but some differences can be seen in comparison to the "standard" simulations of Fig. 3 – for example a slightly faster rate of HBr conversion to reactive bromine. However, this more detailed reaction scheme is itself limited in that it does not include reaction of $BrNO_2$ with Br (rate constant unknown), and assumes that the two possible BrONO photolysis pathways occur equally (as products are unknown). Further, the scheme does not include potential heterogeneous reactions relevant for $BrNO_2$. Heterogeneous reactive uptake of $N_2O_5$ might produce $BrNO_2$ or $ClNO_2$. However, these products might react further within the aerosol to form $Br_2$ or BrCl (Frenzel et al., 1998). Proper investigation of such

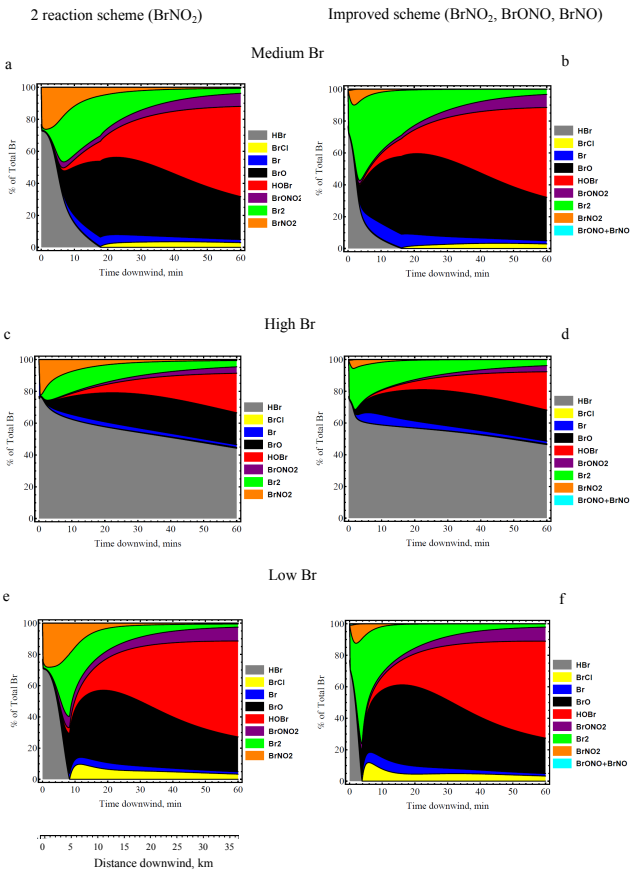


**Figure 5.** Br speciation in model runs that also include formation of $BrNO_2$, shown for the three bromine emission scenarios. Simulations incorporate $BrNO_2$ using a 2-reaction scheme **(a, c, e)** or a 12-reaction scheme including $BrNO_2$, BrONO and BrNO **(b, d, f)**. See text for details.

heterogeneous chemistry on volcanic aerosol would require detailed consideration of the underlying rate constants for all the aqueous-phase reactions (e.g. in a manner similar to that recently attempted for HOBr reactive uptake, Roberts et al., 2014). In addition to uncertainty in the model chemistry, the model findings are also subject to uncertainty in the HSC initialisation (which determines the volcanic Br and $NO_2$ radical source), see Sect. 3.3. Nevertheless, the more detailed reaction $BrNO_2$–BrONO–BrNO scheme findings suggest that the influence of $BrNO_2$ on the plume chemistry is much lower than that proposed by von Glasow (2010). Further simulations of this study therefore do not include $BrNO_2$.

### 3.6 Influence of plume–air mixing on BrO formation and ozone depletion

Here we investigate the role of plume–air mixing on the (low-temperature) halogen chemistry evolution of the downwind plume. A first study investigates small variations as might be expected on a day-to-day basis at Etna. A second study investigates how large variations in the volcanic emission flux

**Table 3.** List of gas-phase and photolytic reactions related to formation of $BrNO_2$, BrONO and BrNO. Reactions listed are used in the – BrONO–BrNO scheme. The two-reaction $BrNO_2$ scheme assumes $BrNO_2$ as the sole product from both Br + $NO_2$ reactions and photolysis of $BrNO_2$ as the only loss pathway. See text for discussion of possible additional heterogeneous pathways.

| Reaction | Rate coefficient | at 285 K |
|---|---|---|
| $Br+NO_2 \rightarrow BrNO_2$ | $\sim 3.8 \times 10^{-13}$ cm$^3$ molec$^{-1}$ s$^{-1}$ | Brökse and Zabel (1998) |
| $Br+NO_2 \rightarrow BrONO$ | $\sim 4.8 \times 10^{-12}$ cm$^3$ molec$^{-1}$ s$^{-1}$ | Brökse and Zabel (1998) |
| $BrONO+Br \rightarrow Br_2+NO_2$ | $2.4 \times 10^{-11}$ cm$^3$ molec$^{-1}$ s$^{-1}$ | Mellouki et al. (1989) |
| $BrONO+NO_2 \rightarrow BrNO_2+NO_2$ | $\sim 2 \times 10^{-16}$ cm$^3$ molec$^{-1}$ s$^{-1}$ (uncertain) | Brökse and Zabel (1998) |
| $BrONO \rightarrow Br+NO_2$ | $\sim 1.2\,s^{-1}$ (at 298 K, 1 atm) | Brökse and Zabel (1998) |
| | $\tau < 1$ s at 298 K | Orlando and Burkholder (2000) |
| $BrONO \rightarrow BrNO_2$ | unknown | – |
| $BrNO_2+Br \rightarrow Br_2+NO_2$ | unknown | – |
| $BrNO_2+NO \rightarrow BrNO+NO_2$ | $2.3 \times 10^{-12}$ Exp[$-17.8$/RT] cm$^3$ molec$^{-1}$ s$^{-1}$ | Brökse and Zabel (1998) |
| $BrONO+NO \rightarrow BrNO+NO_2$ | unknown, larger than $BrNO_2$ equivalent | – |
| $BrNO+Br \rightarrow Br_2+NO$ | $3.7 \times 10^{-10}$ cm$^3$ molec$^{-1}$ s$^{-1}$ | Hippler et al. (1978) |
| | or: $5.2 \times 10^{-12}$ cm$^3$ molec$^{-1}$ s$^{-1}$ | Grimley and Houston (1980) |
| $BrNO_2 \rightarrow Br+NO_2$ | $\leq 4.0 \times 10^{-4}$ s$^{-1}$ | Brökse and Zabel (1998) |
| | $\sim 6.4 \times 10^{-5}$ s$^{-1}$ | |
| $2BrNO_2 \rightarrow Br_2+2NO_2$ | Unknown (slow) | Brökse and Zabel (1998) |
| $BrONO \xrightarrow{h\nu} Br+NO_2$ | $\tau \sim$ s (products unknown) | Burkholder and Orlando (2000) |
| $BrONO \xrightarrow{h\nu} BrO+NO$ | or $\tau \sim$ s (products unknown) | |
| $BrNO_2 \xrightarrow{h\nu} Br+NO_2$ | $\tau \sim$ min | Scheffler et al. (1997) |

(e.g. due to an eruption) influence the plume chemistry, albeit within the limitations of an idealised model scenario.

### 3.6.1 Influence of plume dispersion parameters, volcanic emission flux and wind speed on BrO / $SO_2$

As already discussed in Sect. 3.4, BrO formation is initially promoted by the entrainment of background air (containing ozone, $HO_x$ and $NO_x$), due to the balance between the reaction Br + $O_3$ (Reaction R6) and the self-reaction of BrO (Reaction R7), but as the plume becomes more diluted the entrainment of air acts to reduce BrO / $SO_2$ due to the reaction of BrO with $HO_2$ and $NO_2$ (Reactions R1, R2). Thus, the proportion of background air that has been entrained into the plume acts as a key control on BrO / $SO_2$. In the single-box Gaussian plume dispersion model used here, the extent of mixing of the background air into the plume is controlled by the Pasquill–Gifford dispersion parameters as a function of distance downwind, whose choice depends on atmospheric turbulence (a function of wind speed and atmospheric stability). Further, for a given dispersion parameterisation, the extent of mixing depends inversely on the volcanic emission flux, and also depends on wind speed (through dilution along the plume). Here the effects of these three variables are illustrated for a range of plausible volcanic and meteorological conditions at Etna in Fig. 6.

For the base-run simulations (also shown in Figs. 3 and 4), a Pasquill–Gifford (PG) dispersion case D was used, that is for a relatively neutral atmosphere, with a wind speed of 10 m s$^{-1}$ and volcanic gas flux of 10 kg s$^{-1}$ $SO_2$ (with the emission of all other volcanic gas and aerosol components scaled accordingly). This $SO_2$ flux estimate is close to the $\sim$13 kg s$^{-1}$ reported by McGonigle et al. (2005) for 30 July 2004. The model 10 kg s$^{-1}$ $SO_2$ flux is, however, a somewhat low representation for Mt Etna during 2004–2005 in general. Aiuppa et al. (2005) report gas flux data that show summertime variations between 800 and 2000, equivalent to 9–23 kg s$^{-1}$ $SO_2$, with even greater $SO_2$ flux during eruption periods. Burton et al. (2005) report 7-day average $SO_2$ fluxes of 1000–2500 t d$^{-1}$ (12–25 kg s$^{-1}$). To illustrate the influence of variation gas flux and plume dispersion, simulations were also performed at 20 kg s$^{-1}$ $SO_2$ flux, and for a range of dispersion and wind-speed cases. Cases C and B are introduced for more unstable atmospheric conditions involving enhanced plume–air mixing, which occur more readily at lower wind speed (< 6 m s$^{-1}$) (see Supplement).

Simulations performed at wind speeds of 10 m s$^{-1}$ (case D and C), 15 m s$^{-1}$ (case D and C), 5 m s$^{-1}$ (case D and C), and 3 m s$^{-1}$ (case C and B) are shown in Fig. 6 (a "medium" bromine scenario is assumed for all these simulations, with $V_A : V_M = 5 : 95$ in the initialisation). The model runs illustrate how plume–air mixing may cause variation in the downwind BrO / $SO_2$. The variation is of a similar magnitude to that identified in the model runs with the three bromine scenarios, Fig. 4 (which themselves encompass only a portion of the reported variability in Br / S in the emission, see Aiuppa et al., 2005). The model runs suggest that a combination of

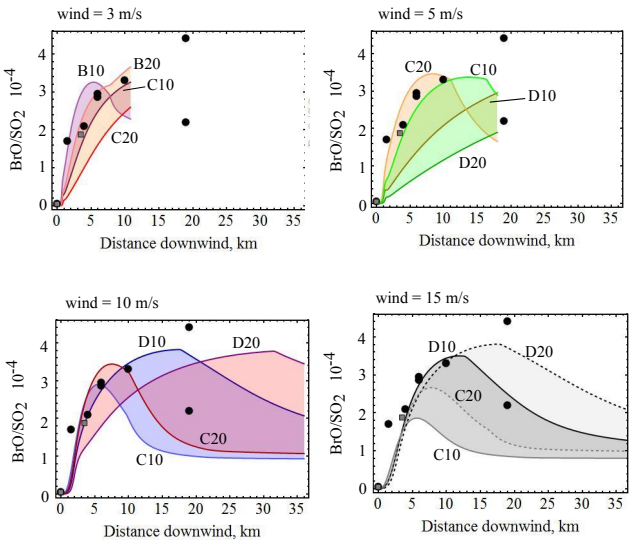


**Figure 6.** Simulated $BrO / SO_2$ over 1 h for the medium bromine emission, predicted for two emission flux scenarios (10 or 20 kg s$^{-1}$), and for a range of wind speeds (3, 5, 10, 15 m s$^{-1}$), and Pasquill–Gifford dispersion schemes (B, C, D). See text for details of the combinations. Model runs are compared to observations from Bobrowski et al. (2007) and Oppenheimer et al. (2006), shown as black circles and grey squares, respectively.

variations in plume–air mixing and bromine emission could provide – at least theoretically – a variability in $BrO / SO_2$ similar to the observed variability in $BrO / SO_2$ ($5. \times 10^{-5} - 3.9 \times 10^{-4}$) reported by Bobrowski and Guiffrida (2012) at 6 km downwind. Variability in the volcanic aerosol emission could potentially add further to this.

Plume dispersion causes a transition between the two chemical regimes outlined above and an intermediate maximum in $BrO / SO_2$. The magnitude and location of the downwind maximum in $BrO / SO_2$ depends on the extent of plume–air mixing, as determined by the gas flux, rate of dispersion and wind speed, as well as on the volcanic aerosol loading and bromine content, and the HSC initialisation. Variations in background atmospheric composition (e.g. ozone, $HO_x$, $NO_x$, aerosol) could further modify the results. Finally, if applying these results to volcanoes elsewhere, the summit altitude is also a relevant consideration, as the greater atmospheric density at lower altitude will yield a higher in-plume ratio of background oxidants to bromine, for a given volcanic $SO_2$ flux.

Nevertheless, large increases in the volcanic emission flux tend to maintain for longer the more "concentrated" regime where $BrO / SO_2$ is limited by the balance between Reactions (R6) and (R7), as discussed further below.

### 3.6.2 Effect of a large increase in volcanic flux on $BrO / SO_2$

The sensitivity study is continued for high-emission scenarios by keeping the plume dispersion case and bromine emission scenario constant (case D, "medium" $Br_{tot} / SO_2$), but increasing the volcanic gas and aerosol emission (by a factor of $\times 5$ and $\times 10$ of the base-run 10 kg s $SO_2$ flux). Such an increased volcanic emission maintains higher concentrations of volcanic gases and thus reduces the extent of plume–air mixing, and hence entrainment of background oxidants into the plume. We caution that in a real volcanic environment, such a large change in degassing rate may also be accompanied by a change in composition of the volcanic emission (including halogen content or aerosol loading) or act to alter the plume dimensions somewhat (e.g. by the dynamics of explosive eruptions). The model results here focus solely on the effect of (substantially) enhanced gas flux with all other variables held constant.

Simulations of 3 h duration (equivalent to 108 km downwind plume propagation assuming 10 m s$^{-1}$ wind speed) with volcanic emission flux increased from the base run to $\times 5$ and $\times 10$ are shown in Fig. 7, for both the "medium" and "high" bromine emission scenarios (initialised with HSC using $V_A : V_M = 5 : 95$). The enhanced volcanic emission flux linearly enhances in-plume $SO_2$ abundance, as expected, but exerts a non-linear effect on the plume chemistry and impacts.

In particular, the greater volcanic emission (lower plume–air mixing) leads to a slower rise, and a later onset and slower decline in $BrO / SO_2$. At distances far downwind (> 2 h for the specific simulation conditions), high $BrO / SO_2$ is sustained for longer in plumes with high gas flux. Conversely, in the near downwind (several 10s of min), plumes with lowest gas flux exhibit the fastest initial rise and highest $BrO / SO_2$ ratios. As described above, these model findings are readily explained by the model chemistry that partitions reactive bromine between Br and BrO (during the initial rise), and BrO, and HOBr, $BrONO_2$ (during the subsequent decline) as the plume disperses. The onset and magnitude of the decline is greatest for low-flux plumes that are more dilute and where a higher proportion of background air has been mixed into the plume. Conversely, high-flux and thus more concentrated plumes have a slower initial increase in $BrO / SO_2$, with a delayed maximum. In the relatively near-downwind plume (0–30 min), the model predicts lower $BrO / SO_2$ at greater volcanic gas fluxes, as shown by the arrows in Fig. 6. Implications for the interpretation of volcano plume observations are discussed in Sect. 3.7.

### 3.6.3 Atmospheric impacts of volcanic reactive halogen chemistry

BrO chemistry causes ozone, $HO_x$ and $NO_x$ to become depleted in the downwind plume, Fig. 8. For $HO_x$ and $NO_x$

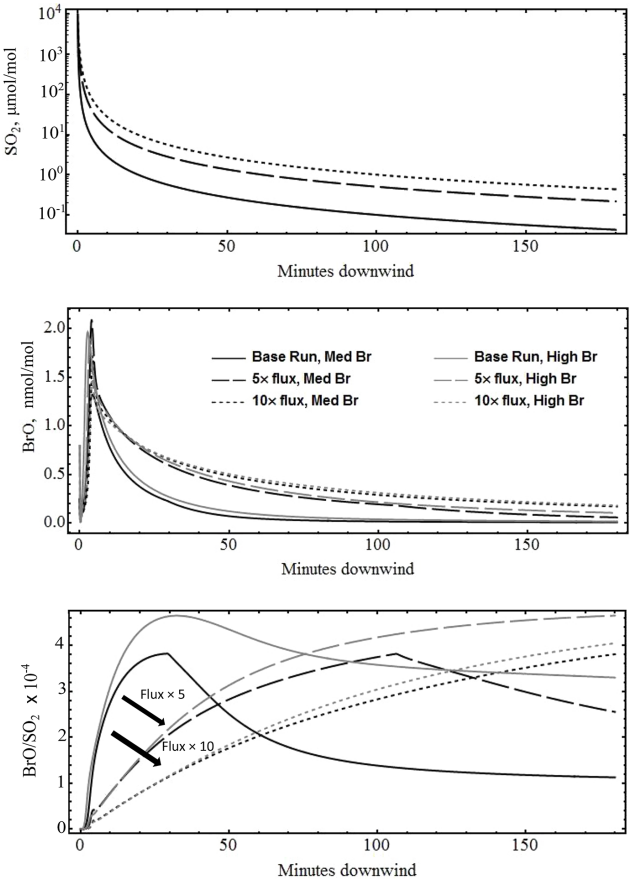


**Figure 7.** Simulated plume $SO_2$, BrO and BrO / $SO_2$ over 3 h for the medium- and high-bromine emission scenarios, and with varying volcanic emission flux (baseline run, and with volcanic gas+aerosol emissions flux × 5 and × 10, shown by full-, long-dashed and short-dashed lines, respectively), whilst keeping the same plume dispersion parameterisation, wind speed and initialisation (see text for model details and interpretation). Arrows highlight the reduction in near-downwind BrO / $SO_2$ predicted at greater volcanic emission flux.

the near-downwind plume abundances are initially elevated as the HSC initialisations used assumed a volcanic source of these species (Fig. 2), but become depleted within a few to 10s of minutes downwind. The maximum depletion reaches is near 100 and > 70 % depletion relative to background values of around 30 and 0.17 ppbv for $HO_x$ and $NO_x$ respectively. $HO_x$ is converted into $H_2O_{(l)}$ via HOBr chemistry (Reactions R1, R3). $HO_x$ abundances are also reduced by the gas-phase reaction of OH with $SO_2$, and by ozone depletion in the plume (see below). The volcanic $NO_x$ source is converted into $HNO_3$ by $BrONO_2$ chemistry (Reactions R2, R4), causing a rapid increase of in-plume $HNO_3$, particularly in the concentrated near-downwind plume, where $HNO_3$ reaches up to 60 nmol mol$^{-1}$ (exceeding the background $NO_y$ of ∼ 6 nmol mol$^{-1}$). This mechanism was proposed by Roberts et al. (2009) as an explanation for observations of high $HNO_3$ in volcanic plumes. See collated observations by Martin et al. (2012) reporting plume $HNO_3$ / $SO_2$ that can reach up to $10^{-1}$. For Etna in particular, reported crater-rim $HNO_3$ / $SO_2$ ratios are somewhat inconsistent and show large variability ($-2.3 \times 10^{-4}$, $7.8 \times 10^{-6}$, $4.2 \times 10^{-3}$), which in itself might be indicative of a role of plume chemistry processing. Recently Voigt et al. (2014) also observed elevated $HNO_3$ in the downwind Etna plume, with $HNO_3$ as the dominant form of $NO_y$. Importantly, elevated "volcanic" $HNO_3$ produced by the $BrONO_2$ mechanism can originate from both $NO_x$ of volcanic origin, and from $NO_x$ from background air entrained into the plume. As a consequence, the in-plume $NO_x$ declines from initially elevated abundance (due to the assumed high-temperature volcanic $NO_x$ source) to become depleted relative to the background abundance downwind. Finally, it is noted that simple acidification of nitrate aerosol from background air entrained into the plume could also lead to gas partitioning and therefore enhance the "volcanic" $HNO_{3(g)}$ signature. Such acid displacement of $HNO_{3(g)}$ by $H_2SO_{4(aq)}$ has been observed by Satsumabayashi et al. (2004). The observations of volcanic $HNO_3$ collated by Martin et al. (2012) and Voigt et al. (2014) thus require consideration in the context of these two mechanisms.

Ozone is also depleted in the plume and reaches a maximum depletion (up to 100 %) around 10 min downwind, coincident with the highest in situ BrO abundances that reach ∼ 1 nmol mol$^{-1}$ (Fig. 7). For the base run, the maximum plume ozone depletion is 30 or 45 nmol mol$^{-1}$ for the medium- and high-bromine emission scenarios respectively. Greater in-plume ozone loss occurs at higher emissions flux (lower relative plume–air mixing). However, for these runs the maximum ozone loss is constrained by the fact that it cannot exceed ∼ 60 nmol mol$^{-1}$ (the background ozone mixing ratio). Thereafter ozone begins to recover as the plume disperses (Fig. 8), entraining background air, and BrO declines (Fig. 7), albeit at a slower rate than the $SO_2$ plume tracer. Ozone recovery is greater for the base run than the higher volcanic flux cases due to both physical and chemical consequences of enhanced plume–air mixing. Thus the presence of a detectable ozone depletion signature at distances far downwind depends on the emission flux and plume dispersion. Further, the single-box simulations presented here that predict the downwind trend do not simulate the ozone distribution across the plume cross section. Ozone loss is typically greater in the plume centre than near the edges, as demonstrated by both observations and spatially resolved PlumeChem simulations of Redoubt volcano plume (Kelly et al., 2013). The single-box simulations should be interpreted in this context, e.g. a predicted loss of 45 nmol mol$^{-1}$ implies greater loss at the plume centre (likely close to 60 nmol mol$^{-1}$ or 100 %) declining to near-ambient ozone at the plume edges. With distance (time) downwind, the ozone mixing ratio starts to increase when the entrainment of ambient air containing $O_3$ is faster than

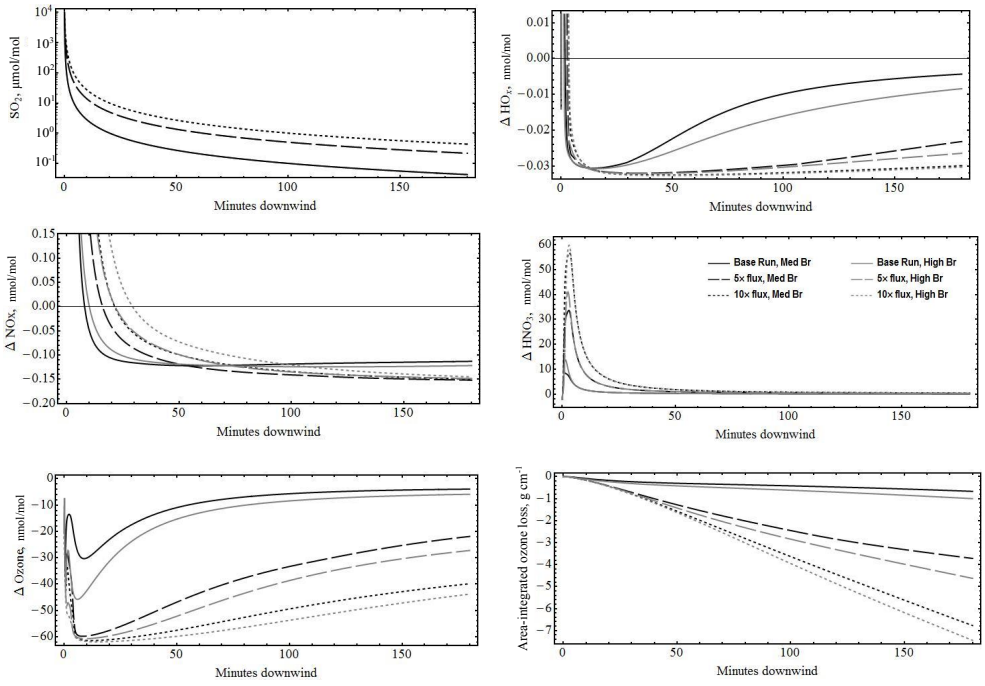


**Figure 8.** Simulated impact of plume BrO chemistry on atmospheric oxidants, shown for the model scenarios of Fig. 7. Depletion of oxidants and formation of $NO_y$ is shown through the difference in plume – background mixing ratio for $HO_x$ ($OH+HO_2$), $NO_x$ ($NO+NO_2$), $HNO_3$, and ozone. Cumulative ozone loss is also calculated across the 3 h simulations.

the local $O_3$ destruction (Fig. 8). Nevertheless, ongoing occurrence of ozone-depleting BrO chemistry is demonstrated by the continuing negative trend in the cumulative ozone loss: the ozone difference (plume – background) integrated across the plume cross-sectional area declines along the 3 h simulations to reach $\sim 1$, 4, and 7 g cm$^{-1}$ for the three flux scenarios ($SO_2$ flux = 10, 50, 100 kg s$^{-1}$) respectively with greater ozone loss for the high Br compared to the medium Br scenario, as expected. These Lagrangian simulations of plume "puff" ozone evolution over 3 h can also be viewed in an Eulerian context: the 3 h impact of continuous volcano emissions is calculated by integrating the cross-sectional impact (g cm$^{-1}$) over the distance downwind. This yields ozone losses of $35 \times 10^3$ ($38 \times 10^3$), $23 \times 10^3$ ($26 \times 10^3$), and $4 \times 10^3$ ($6 \times 10^3$) kg for the $\times$ 10 flux, $\times$ 5 flux and base-run (10 kg s$^{-1}$ $SO_2$ flux) scenarios respectively, assuming the medium Br scenario (numbers in brackets refer to high Br scenario). Whilst there is some linearity in ozone loss per Br emitted (e.g. in comparing the base run to $\times$ 5 flux cases), the constraint that ozone loss cannot exceed 100 % of the background abundance introduces some non-linearity for the $\times$ 10 flux case, thereby reducing its overall ozone loss. Note that the plume cross-sectional area after 3 h is $\pi \times \sqrt{2} \times \sigma_h \times \sqrt{2} \times \sigma_z = 2 \times \pi \times 4470 \times 485 = 1.4 \times 10^7$ m$^2$. The volcanic plume cone thus resides within a cylinder of volume $1.4 \times 10^7 \times 108 \times 10^3 = 1.5 \times 10^{12}$ m$^3$, containing approx. $10^5$ kg ozone.

Figure 8 indicates that the plume atmospheric impacts extend beyond the 1 to 3 h simulations presented in this study. Simulations over the lifetime of volcanic plumes under different volcanological and meteorological conditions are therefore required to quantify the global tropospheric impact from volcanic halogen emissions.

### 3.7 Implications for modelling and observations of volcanic BrO

The parameter space governing volcanic plume reactive halogen chemistry is vast, and is not fully constrained by available observations. Of particular importance in controlling the reactive bromine formation and downwind plume bromine speciation are: $Br_{tot}$ / $SO_2$ in the emission, the volcanic aerosol loading, and the extent of background air mixing into the plume (itself a function of the plume dispersion parameterisation, volcanic emission flux and wind speed). These factors exert non-linear influences on the conversion of emitted HBr into plume reactive bromine, and its speciation through interconversion of BrO, Br, $Br_2$, BrCl, HOBr, $BrONO_2$.

The onset of the autocatalytic reactive bromine formation is also accelerated in the model by radicals in the high-temperature model initialisation (Br, Cl, $NO_x$, $HO_x$). A major area of uncertainty is, however, the representation of this high-temperature near-vent plume environment using thermodynamic models such as HSC. Development of

high-temperature kinetic models of the near-vent plume is encouraged for progress in this area.

Further uncertainty to the downwind plume chemistry is contributed by uncertainty in the volcanic bromine emission, and in aerosol surface area, that sustains halogen cycling downwind. Crater-rim filter-pack measurements (e.g. Aiuppa et al., 2005) provide estimates of volcanic Br / S emissions for model initialisation (see Table 2) but also highlight temporal variability in this parameter. The volcanic aerosol emission is poorly constrained by observations at Etna, and from volcanoes globally. A surface area loading of $\sim 10^{-11}$ µm$^2$ molec $SO_2^{-1}$, i.e. an order of magnitude lower than that used by Roberts et al. (2009), yields simulated (0–20 km) downwind $BrO / SO_2$ more consistent with that observed in the Etna plume. Volcanic aerosol has a small influence on $BrO / SO_2$ ratio near source, but is an important control in the more dispersed plume downwind. Uncertainties in the volcanic aerosol emission magnitude, and its size distribution (which for sulfate varies as a function of temperature and humidity) thus contribute to uncertainties in models of the plume halogen chemistry. Plume aerosol may be augmented by in-plume oxidation of volcanic $SO_2$ to $H_2SO_4$, and the entrainment and acidification of background aerosol may also promote halogen cycling. Future model evaluation of volcanic reactive halogen impacts in the wider troposphere will require the development of regional and global models, with detailed treatment of aerosol processes as well as plume dispersion (shown to be a key control on the downwind chemistry). An improved quantification of the kinetics of HOBr reactive uptake on volcanic aerosol is also needed according to Roberts et al. (2014). Global models may need to include a representation of the subgrid-scale volcanic plume processes, particularly as this study has highlighted how the proportion of emitted HBr converted into reactive forms is non-linearly dependent on the degassing scenario.

We emphasise the complex role of plume chemistry in the interpretation of volcano flank DOAS measurements of $BrO / SO_2$. Bobrowski and Giuffrida (2012) recently reported variation in $BrO / SO_2$ ratios at Etna related to the onset of eruption activity, for example with increasing $BrO / SO_2$ shortly prior to an eruptive event, and lower $BrO / SO_2$ during the eruption event, according to DOAS measurements 6 km downwind from the summit. These observations have been interpreted in the context of variable bromine and $SO_2$ emissions, related to subsurface magmatic processes. Lübcke et al. (2014) identified a decrease in $BrO / SO_2$ observed using a DOAS instrument prior to an eruption event at Nevado del Ruiz, Colombia (in a period whilst $SO_2$ emissions were increasing). However, we emphasise that a variation in plume $BrO / SO_2$ can also result from differences in the plume chemistry for varying volcanic emission flux magnitudes. Figure 6 shows that changes in volcanic gas flux (for a fixed plume dimension) can yield substantial changes in plume $BrO / SO_2$ ratio, even for a fixed $Br_{tot} : SO_2$ ratio in the emission. In the near-downwind plume, a key control on BrO formation is the entrainment of oxidants. A substantial increase in volcanic emission flux leads to greater plume strength and reduced ratio of background oxidants to bromine in the model. Thus, on the < 60 min timescale of volcano flank DOAS observations, a substantially enhanced rate of volcanic degassing generally leads to lower plume $BrO / SO_2$ ratios in more concentrated plumes. Potentially, the variations in $BrO / SO_2$ identified by Bobrowski and Giuffrida (2012), and Lübcke et al. (2014) may result from a combination of volcanological and plume chemistry factors. This example highlights the complexity surrounding the interpretation of volcanic BrO and shows the role of plume chemistry modelling in the effort to use volcanic BrO observations to monitor and predict volcanic activity.

We also highlight that the plume chemical evolution causes a decline in $BrO / SO_2$ ratios in the dispersed plume further downwind through net conversion of BrO into reservoirs such as HOBr and $BrONO_2$. This plume chemical evolution acts to reduce the BrO column abundance, contributing additional limitations to its possible detection in dispersed plumes, and is the model explanation for the plateau in $BrO / SO_2$ downwind of Etna reported by Bobrowski and Guiffrida (2012). Detection of volcanic BrO by satellite is primarily constrained to large volcanic emissions (Theys et al., 2009; Rix et al., 2012; Hörmann et al., 2013). Smaller volcanic emissions that generate high but localised BrO at lower altitudes are less readily detected, particularly due to dilution effects across the satellite measurement pixel (Afe et al., 2004). The modelled plume chemical evolution adds to this limitation for satellite detection of BrO in dispersed volcanic plumes (even at higher resolution). Importantly, however, the model Br speciation shows that a declining trend in BrO abundance as the volcanic plume disperses does not preclude the occurrence of continued in-plume reactive bromine chemistry as predicted by the model.

## 4 Conclusion

We present a *PlumeChem* model study of the reactive halogen chemistry of Mt Etna volcano plume that reproduces the recently reported trends in $BrO / SO_2$; namely a rapid increase in the near-downwind followed by stability or decline in the far-downwind plume. A new in-plume evolution of Br speciation is predicted: BrO $Br_2$, Br and HBr are the main plume species in the near-downwind plume whilst BrO, HOBr (and $BrONO_2$, BrCl) are present in significant quantities further downwind. An evaluation of the (quantifiable) chemistry surrounding $BrNO_2$ suggests a rather low prevalence in volcanic plumes, although uncertainties in model chemistry and initialisation are highlighted.

Emitted volcanic HBr is converted into reactive bromine by autocatalytic bromine chemistry cycles whose onset is accelerated by the model high-temperature initialisation. The initial rise in $BrO / SO_2$ is primarily due to entrainment of

ozone through plume dispersion that promotes BrO formation from Br radicals. A subsequent decline or plateau in $BrO / SO_2$ occurs upon plume dispersion, which both dilutes the volcanic aerosol (slowing HOBr and $BrONO_2$ heterogeneous loss rates) and entrains $HO_2$ and $NO_2$ from the background atmosphere (promoting HOBr and $BrONO_2$ formation from BrO). This promotes net accumulation of reservoirs HOBr and $BrONO_2$ and a reduction in BrO in the dispersed downwind plume. Thus the model can explain the reported $BrO / SO_2$ trend at Etna. We demonstrate the role of plume chemistry models to interpret volcanic $BrO / SO_2$ observations as well as quantify atmospheric impacts on $HO_x$, $NO_x$, $HNO_3$ and ozone. A number of volcanological and meteorological factors can influence plume $BrO / SO_2$ ratios, and we illustrate simulations with contrasting total bromine content and volcanic aerosol loading. The influence of plume–air mixing is shown by simulations with varying dispersion rate, as well as wind speed and volcanic gas flux.

BrO contents reach up to 20 and $\sim 50$ % of total bromine (over a timescale of a few 10s of minutes), for the high- and medium-/low-bromine emission scenarios, respectively. The latter agrees well with observations that report BrO (at 3–5 min downwind) can reach up to 40 % of the total bromine emission at Etna (Oppenheimer et al., 2006). Partial (up to $\sim 50$ %) or complete (100 %) conversion of HBr to reactive forms is predicted over the 1 h simulations, depending on bromine content (high, medium or low, respectively) as well as other the plume conditions (e.g. aerosol, dispersion, HSC initialisation). Simulations using the two volcanic aerosol loadings significantly differ in the downwind plume chemistry but result in a similar initial rise in $BrO / SO_2$ near-downwind (up to 6 km), a finding that is in agreement with the reported low relative humidity dependence of $BrO / SO_2$ (Bobrowski and Giuffrida, 2012).

Simulations with a fixed dispersion rate but enhanced volcanic emission flux are presented. For higher emission fluxes, the stronger plume and reduced ratio of background oxidants to bromine causes a slower rise in $BrO / SO_2$ in the near-downwind plume ($< 40$ min) and a slower and delayed onset of the decrease in $BrO / SO_2$ in the far-downwind plume ($> 2$ h, for the volcanic conditions simulated). This simulated dependence of $BrO / SO_2$ on volcanic emission flux (albeit in an idealised model scenario) is particularly relevant for the interpretation of changes in $BrO / SO_2$ during/prior to eruptive events (e.g. Bobrowski and Giuffrida, 2012; Lübcke et al., 2014).

Impacts of the plume halogen chemistry include downwind depletion of $HO_x$, $NO_x$ and ozone, and formation of $HNO_3$. Partial recovery of ozone is predicted, particularly for low gas flux emissions. However, cumulative impacts on ozone are ongoing over the 3 h simulations.

**The Supplement related to this article is available online at doi:10.5194/acp-14-11201-2014-supplement.**

*Author contributions.* T. J. Roberts, designed and performed the *PlumeChem* model experiments and HSC calculations and wrote the manuscript. R. S. Martin advised on HSC methodology and contributed to manuscript writing. L. Jourdain advised on scientific scope and contributed to manuscript writing.

*Acknowledgements.* This study was financed by LABEX VOLTAIRE (VOLatils-Terre Atmosphère Interactions – Ressources et Environnement) ANR-10-LABX-100-01 (2011–20) and an NSINK career development allowance that enabled HSC software purchase. R. S. Martin acknowledges Christ's College, Cambridge for a research fellowship. We are grateful to R. Sander, C. Kern and an anonymous reviewer, whose feedback helped to improve the manuscript.

Edited by: W. Birmili

## References

Afe, O. T., Richter, A., Sierk, B., Wittrock, F., and Burrows, J. P.: BrO emission from volcanoes: A survey using GOME and SCIAMACHY measurements, Geophys. Res. Lett., 31, L24113, doi:10.1029/2004GL020994, 2004.

Aiuppa, A., Federico, C., Franco, A., Giudice, G., Guierri, S., Inguaggiato, S., Liuzzo, M., McGonigle, A. J. S., and Valenza, M.: Emission of bromine and iodine from Mount Etna volcano, Geochem. Geophy. Geosy., 6, Q08008, doi:10.1029/2005GC000965, 2005.

Aiuppa, A., Shinohara, H., Tamburello, G., Giudice, G., Liuzzo, M., and Moretti, R.: Hydrogen in the gas plume of an open-vent volcano, Mount Etna, Italy, J. Geophys. Res., 116, B10204, doi:10.1029/2011JB008461, 2011.

Bagnato, E., Aiuppa, A., Parello, F., Calabrese, S., D'Alessandro, W., Math, T. A., McGonigle, A. J. S., Pyle, D. M., and Wangberg, I.: Degassing of gaseous (elemental and reactive) and particulate mercury from Mount Etna volcano (Southern Italy), Atmos. Environ., 41, 7377–7388, 2007.

Baker, A. K., Rauther-Schöch, A., Schuck, T. J., Brenninkmeijer, C. A. M., van Velthoven, P. F. J., Wisher, A., and Oram, D. E.: Investigation of chlorine radical chemistry in the Eyjafjallajökull volcanic plume using observed depletions in non-methane hydrocarbons, Geophys. Res. Lett., 38, L13801, doi:10.1029/2011GL047571, 2011.

Bani, P., Oppenheimer, C., Tsanev, V. I., Carn, S. A., Cronin, S. J., Crimp, R., Calkins, J. A., Charley, D., Lardy, M., and Roberts, T. J.: Surge in sulphur and halogen degassing from Ambrym volcano, Vanuatu, B. Volcanol., 71, 1159–1168, doi:10.1007/s00445-009-0293-7, 2009.

Bobrowski, N., Honniger, G., Galle, B., and Platt, U.: Detection of bromine monoxide in a volcanic plume, Nature, 423, 273–276, doi:10.1038/nature01625, 2003.

Bobrowski, N. and Platt, U.: $SO_2$/BrO ratios studied in five volcanic plumes, J. Volcanol. Geoth. Res., 166, 1470–160, doi:10.1016/j.jvolgeores.2007.07.003, 2007.

Bobrowski, N., von Glasow, R., Aiuppa, A., Inguaggiato, S., Louban, I., Ibrahim, O. W., and Platt, U.: Reactive halogen chemistry in volcanic plumes, J. Geophys. Res., 112, D06311, doi:10.1029/2006JD007206, 2007.

Bobrowski, N. and Giuffrida, G.: Bromine monoxide / sulphur dioxide ratios in relation to volcanological observations at Mt. Etna 2006–2009, Solid Earth, 3, 433–445, doi:10.5194/se-3-433-2012, 2012.

Boichu, M., Oppenheimer, C., Roberts, T. J., Tsanev, V., and Kyle, P. R.: On bromine, nitrogen oxides and ozone depletion in the tropospheric plume of Erebus volcano (Antarctica), Atmos. Environ., 45, 3856–3866, 2011.

Bröske R. and Zabel, F.: Kinetics of the Gas-Phase Reaction of $BrNO_2$ with NO, J. Phys. Chem. A, 102, 8626–8631, 1998.

Burkholder, J. B. and Orlando, J. J.: UV absorption cross-sections of cis-BrONO, Chem. Phys. Lett., 317, 603–608, 2000.

Burton, M. R., Neri, M., Andronico, D., Branca, S., Caltabiano, T., Calvari, S., Corsaro, R. A., Del Carlo, P., Lanzafame, G., Lodato, L., Miraglia, L., Salerno, G., and Spampinato, L.: Etna 2004–2005: An archetype for geodynamically-controlled effusive eruptions, Geophys. Res. Lett., 32, L09303, doi:10.1029/2005GL022527, 2005.

Carn, S. A, Froyd, K. D., Anderson, B. E., Wennberg, P., Crounse, J., Spencer, K., Dibb, J. E., Krotkov, N. A., Browell, E. V., Hair, J. W., Diskin, G., Sachse, G., and Vay, S. A.: In situ measurements of tropospheric volcanic plumes in Ecuador and Colombia during TC, J. Geophys. Res., 116, D00J24, doi:10.1029/2010JD014718, 2011.

Frenzel, A., Scheer, V., Sikorski, R., George, C., Behnke, W., and Zetzsch, C.: Heterogeneous Interconversion Reactions of $BrNO_2$, $ClNO_2$, $Br_2$, and $Cl_2$, J. Phys. Chem. A, 102, 1329–1337, 1998.

Gerlach, T. M.: Volcanic sources of tropospheric ozone-depleting trace gases, Geochem. Geophys. Geosy., 5, Q09007, doi:10.1029/2004GC000747, 2004.

Giggenbach, W. F.: Redox processes governing the chemistry of fumarolic gas discharges from White Island, New Zeland, Appl. Geochem., 2, 143–161, 1987.

Grimley, A. J. and Houston, P. L.: The photochemistry of nitrosyl halides: The X+NOX–> X2+NO(v) reaction (X = Cl, Br), J. Chem. Phys., 72, 1471, doi:10.1063/1.439371, 1980.

Heue, K.-P., Brenninkmeijer, C. A. M., Baker, A. K., Rauthe-Schöch, A., Walter, D., Wagner, T., Hörmann, C., Sihler, H., Dix, B., Frieß, U., Platt, U., Martinsson, B. G., van Velthoven, P. F. J., Zahn, A., and Ebinghaus, R.: $SO_2$ and BrO observation in the plume of the Eyjafjallajökull volcano 2010: CARIBIC and GOME-2 retrievals, Atmos. Chem. Phys., 11, 2973–2989, doi:10.5194/acp-11-2973-2011, 2011.

Hippler, H., Luu, S. H., Teitelbaum, H., and Troe, J.: Flash photolysis study of the NO-catalyzed recombination of bromine atoms, Int. J. Chem. Kinet., 10, 155–169, 1978.

Hobbs, P. V., Tuell, J. P., Hegg, D. A., Radke, L. F., and Eltgroth, M. W.: Particles and gases in the emissions from the 1980–1981 volcanic eruptions of Mt. St. Helens., J. Geophys. Res., 87, 11062–11086, 1982.

Hörmann, C., Sihler, H., Bobrowski, N., Beirle, S., Penning de Vries, M., Platt, U., and Wagner, T.: Systematic investigation of bromine monoxide in volcanic plumes from space by using the GOME-2 instrument, Atmos. Chem. Phys., 13, 4749–4781, doi:10.5194/acp-13-4749-2013, 2013.

Kelly, P. J., Kern, C., Roberts, T. J., Lopez, T., Werner, C., and Aiuppa, A.: Rapid chemical evolution of tropospheric volcanic emissions from Redoubt Volcano, Alaska, based on observations of ozone and halogen-containing gases, Journal of Volcanology and Geothermal Research, J. Volcanol. Geoth. Res., 259, 317–333, 2013.

Kern, C., Sihler, H., Vogel, L., Rivera, C., Herrera, M., and Platt, U.: Halogen oxide measurements at Masaya Volcano, Nicaragua using active long path differential optical absorption spectroscopy, B. Volcanol., 71, 659–670, 2009.

Kern, C., Deutschmann, T., Werner, C., Sutton, A. J., Elias, T., and Kelly, P. J.: Improving the accuracy of $SO_2$ column densities and emission rates obtained from upward-looking UV-spectroscopic measurements of volcanic plumes by taking realistic radiative transfer into account, J. Geophys. Res., 117, D20302, doi:10.1029/2012JD017936, 2012.

Louban, I., Bobrowski, N., Rouwet, D., Inguaggiato, S., and Platt, U.: Imaging DOAS for volcanological applications, B. Volcanol., 71, 753–765, 2009.

Lübcke, P., Bobrowski, N., Arellano, S., Galle, B., Garzón, G., Vogel, L., and Platt, U.: $BrO / SO_2$ molar ratios from scanning DOAS measurements in the NOVAC network, Solid Earth, 5, 409–424, doi:10.5194/se-5-409-2014, 2014.

Martin, R. S., Mather, T. A., and Pyle, D. M.: High-temperature mixtures of magmatic and atmospheric gases, Geochem. Geophy. Geosy., 7, Q04006, doi:10.1029/2005GC001186, 2006.

Martin, R. S., Roberts, T. J., Mather, T. A., and Pyle, D. M.: The implications of $H_2S$ and $H_2$ stability in high-T mixtures of magmatic and atmospheric gases for the production of oxidized trace species (e.g., BrO and $NO_x$), Chem. Geol., 263, 143–150, 2009.

Martin, R. S., Mather, T. A., Pyle, D. M., Power, M. Allen, A. G., Aiuppa, A., Horwell, C. J., and Ward E. P. W.: Composition-resolved size distributions of volcanic aerosols in the Mt. Etna plumes, J. Geophys. Res., 113, D17211, doi:10.1029/2007JD009648, 2008.

Martin, R. S., Ilyinskaya, E., and Oppenheimer, C.: The enigma of reactive nitrogen in volcanic emissions, Geochim. Cosmochim. Ac., 95, 93–105, 2012.

Mather, T. A., Allen, A. G., Oppeneheimer, C., Pyle, D. M., and McGonigle, A. J. S.: Size-Resolved Characterisation of Soluble Ions in the Particles in the Tropospheric Plume of Masaya Volcano, Nicaragua: Origins and Plume Processing, J. Atmos. Chem., 46, 207–237, 2003.

Mather, T. A., Pyle, D. M., and Allen, A. G.: Volcanic source for fixed nitrogen in the early Earth's atmosphere, Geology, 32, 905–908, doi:10.1130/G20679.1, 2004.

McGonigle, A. J. S., Inguaggiato, S., Aiuppa, A., Hayes, A. R., and Oppenheimer, C.: Accurate measurement of volcanic $SO_2$ flux: Determination of plume transport speed and integrated $SO_2$ concentration with a single device, Geochem. Geophys. Geosyst., 6, Q02003, doi:10.1029/2004GC000845, 2005.

Mellouki, A., Laverdet, G., Jourdain, J. L., and Poulet, G.: Kinetics of the reactions Br + $NO_2$ + M and I + $NO_2$+ M, Int. J. Chem. Kinet., 21, 1161–1172, doi:10.1002/kin.550211209, 1989.

Metrich, N. and Rutherford, M. J.: Low pressure crystallization paths of $H_2O$-saturated basaltic-hawaiitic melts from Mt Etna: Implications for open-system degassing of basaltic volcanoes, Geochim. Cosmochim. Ac., 62, 1195–1205, 1998.

Millard, G. A., Mather, T. A., Pyle, D. M., Rose, W. I., and Thornton, B.: Halogen emissions from a small volcanic eruption: Modeling the peak concentrations, dispersion, and volcanically in-

duced ozone loss in the stratosphere, Geophys. Res. Lett., 33, L19815, doi:10.1029/2006GL026959, 2006.

Oppenheimer, C., Tsanev, V. I., Braban, C. F., Cox, R. A., Adams, J. W., Aiuppa, A., Bobrowski, N., Delmelle, P., Barclay, J., and McGonigle, A. J. S.: BrO formation in volcanic plumes, Geochim. Cosmochim. Ac., 70, 2935–2941, 2006.

Oppenheimer, C., Kyle, P., Eisele, F., Crawford, J., Huey, G., Tanner, D., Saewung, K., Mauldin, L., Blake, D., Beyersdorf, A., Buhr, M., and Davis, D.: Atmospheric chemistry of an Antarctic volcanic plume, J. Geophys. Res., 115, D04303, doi:10.1029/2009JD011910, 2010.

Orlando, J. J. and Burkholder, J. B.: Identification of BrONO as the Major Product in the Gas-Phase Reaction of Br with $NO_2$, J. Phys. Chem. A, 104, 2048–2053, doi:10.1021/jp993713g, 2000.

Orlando, J. J. and Tyndall, G. S.: Rate coefficients for the thermal decomposition of $BrONO_2$ and the heat of formation of $BrONO_2$, J. Phys. Chem., 100, 19398–19405, 1996.

Rix, M., Valks, P., Hao, N., Loyola, D., Schlager, H., Huntrieser, H., Flemming, J., Koehler, U., Schumann, U., and Inness, A.: Volcanic $SO_2$, BrO and plume height estimations using GOME-2 satellite measurements during the eruption of Eyjafjallajökull in May 2010, J. Geophys. Res., 117, D00U19, doi:10.1029/2011JD016718, 2012.

Roberts, T. J., Braban, C. F., Martin, R. S., Oppenheimer, C., Adams, J. W., Cox, R. A., Jones, R. L., and Griffiths., P. T, Modelling reactive halogen formation and ozone depletion in volcanic plumes, Chem. Geol., 263, 151–163, 2009.

Roberts, T. J., Braban, C. F., Martin, R. S., Oppenheimer, C., Dawson, D. H., Griffiths, P. T. G, Cox, R. A., Saffell, J. R., and Jones, R. L.: Electrochemical Sensing of Volcanic Plumes, Chem. Geol., 332–333, 74–91, 2012.

Roberts, T. J., Jourdain, L., Griffiths, P. T., and Pirre, M.: Reevaluating the reactive uptake of HOBr in the troposphere with implications for the marine boundary layer and volcanic plumes, Atmos. Chem. Phys., 14, 11185–11199, doi:10.5194/acp-14-11185-2014, 2014.

Rose, W. I., Millard, G. A., Mather, T. A., Hunton, D. E., Anderson, B., Oppenheimer, C., Thornton, B. F., Gerlach, T. M., Viggiano, A. A., Kondon, Y., Miller, T. M., and Ballenthin, J. O.: Atmospheric chemistry of a 33–34 hour old volcanic cloud from Hekla Volcano (Iceland): Insights from direct sampling and the application of chemical box modeling, J. Geophys. Res., 111, D20206, doi:10.1029/2005JD006872, 2006.

Satsumabayashi, H., Kawamura, M., Katsuno, T., Futaki, K., Murano, K., Carmichael, G. R., Kajino, M., Horiguchi, M., and Ueda, H.: Effects of Miyake volcanic effluents on airborne particles and precipitation in central Japan, J. Geophys. Res., 109, D19202, doi:10.1029/2003JD004204, 2004.

Scheffler, D., Grothe, H., Willner, A., Frenzel, A., and Zetzsch, C.: Properties of Pure Nitryl Bromide. Thermal Behavior, UV/Vis and FTIR Spectra, and Photoisomerization to trans-BrONO in an Argon Matrix, Inorg. Chem., 36, 335–338, 1997.

Schumann, U., Weinzierl, B., Reitebuch, O., Schlager, H., Minikin, A., Forster, C., Baumann, R., Sailer, T., Graf, K., Mannstein, H., Voigt, C., Rahm, S., Simmet, R., Scheibe, M., Lichtenstern, M., Stock, P., Rüba, H., Schäuble, D., Tafferner, A., Rautenhaus, M., Gerz, T., Ziereis, H., Krautstrunk, M., Mallaun, C., Gayet, J.-F., Lieke, K., Kandler, K., Ebert, M., Weinbruch, S., Stohl, A., Gasteiger, J., Groß, S., Freudenthaler, V., Wiegner, M., Ansmann, A., Tesche, M., Olafsson, H., and Sturm, K.: Airborne observations of the Eyjafjalla volcano ash cloud over Europe during air space closure in April and May 2010, Atmos. Chem. Phys., 11, 2245–2279, doi:10.5194/acp-11-2245-2011, 2011.

Simpson, W. R., von Glasow, R., Riedel, K., Anderson, P., Ariya, P., Bottenheim, J., Burrows, J., Carpenter, L. J., Frieß, U., Goodsite, M. E., Heard, D., Hutterli, M., Jacobi, H.-W., Kaleschke, L., Neff, B., Plane, J., Platt, U., Richter, A., Roscoe, H., Sander, R., Shepson, P., Sodeau, J., Steffen, A., Wagner, T., and Wolff, E.: Halogens and their role in polar boundary-layer ozone depletion, Atmos. Chem. Phys., 7, 4375–4418, doi:10.5194/acp-7-4375-2007, 2007.

Theys, N., Van Roozendael, M., Dils, B., Hendrick, F., Hao, N., and De Mazière, M.: First satellite detection of volcanic bromine monoxide emission after the Kasatochi eruption, Geophys. Res. Lett., 36, L03809, doi:10.1029/2008GL036552, 2009.

Vance, A., McGonigle, A. J. S., Aiuppa, A., Stith, J. L. , Turnbull, K., and von Glasow, R.: Ozone depletion in tropospheric volcanic plumes, Geophy. Res. Lett., 37, L22802, doi:10.1029/2010GL044997, 2010.

Voigt, C., Jessberger, P., Jurkat, T., Kaufmann, S., Baumann, R., Schlager, H., Bobrowski, N., Giuffrida, G., and Salerno, G.: Evolution of $CO_2$, $SO_2$, HCl, and $HNO_3$ in the volcanic plumes from Etna, Geophys. Res. Lett., 41, 2196–2203, doi:10.1002/2013GL058974, 2014.

von Glasow, R.: Atmospheric Chemistry in Volcanic Plumes, P. Natl. Acad. Sci, USA, 107, 6594–6599, 2010.

von Glasow, R., Bobrowski, N., and Kern, C.: The effects of volcanic eruptions on atmospheric chemistry, Chem. Geol., 263, 131–142, 2009.

Wang, T. X., Kelley, M. D., Cooper, J. N., Beckwith, R. C., and Margerum, D. W: Equilibrium, kinetic and UV-spectral characteristics of aqueous bromine chloride, bromine and chlorine species, Inorg. Chem., 33, 5872–5878 , 1994.